

NASA/CR-2009-215566



Nondestructive Evaluation of Advanced Fiber Reinforced Polymer Matrix Composites

A Technology Assessment

*H. Thomas Yolken and George A. Matzkanin
Texas Research Institute, Austin, Texas*

February 2009

NASA STI Program . . . in Profile

Since its founding, NASA has been dedicated to the advancement of aeronautics and space science. The NASA scientific and technical information (STI) program plays a key part in helping NASA maintain this important role.

The NASA STI program operates under the auspices of the Agency Chief Information Officer. It collects, organizes, provides for archiving, and disseminates NASA's STI. The NASA STI program provides access to the NASA Aeronautics and Space Database and its public interface, the NASA Technical Report Server, thus providing one of the largest collections of aeronautical and space science STI in the world. Results are published in both non-NASA channels and by NASA in the NASA STI Report Series, which includes the following report types:

- **TECHNICAL PUBLICATION.** Reports of completed research or a major significant phase of research that present the results of NASA programs and include extensive data or theoretical analysis. Includes compilations of significant scientific and technical data and information deemed to be of continuing reference value. NASA counterpart of peer-reviewed formal professional papers, but having less stringent limitations on manuscript length and extent of graphic presentations.
- **TECHNICAL MEMORANDUM.** Scientific and technical findings that are preliminary or of specialized interest, e.g., quick release reports, working papers, and bibliographies that contain minimal annotation. Does not contain extensive analysis.
- **CONTRACTOR REPORT.** Scientific and technical findings by NASA-sponsored contractors and grantees.
- **CONFERENCE PUBLICATION.** Collected papers from scientific and technical conferences, symposia, seminars, or other meetings sponsored or co-sponsored by NASA.
- **SPECIAL PUBLICATION.** Scientific, technical, or historical information from NASA programs, projects, and missions, often concerned with subjects having substantial public interest.
- **TECHNICAL TRANSLATION.** English-language translations of foreign scientific and technical material pertinent to NASA's mission.

Specialized services also include creating custom thesauri, building customized databases, and organizing and publishing research results.

For more information about the NASA STI program, see the following:

- Access the NASA STI program home page at <http://www.sti.nasa.gov>
- E-mail your question via the Internet to help@sti.nasa.gov
- Fax your question to the NASA STI Help Desk at 443-757-5803
- Phone the NASA STI Help Desk at 443-757-5802
- Write to:
NASA STI Help Desk
NASA Center for AeroSpace Information
7115 Standard Drive
Hanover, MD 21076-1320

NASA/CR-2009-215566



Nondestructive Evaluation of Advanced Fiber Reinforced Polymer Matrix Composites

A Technology Assessment

*H. Thomas Yolken and George A. Matzkanin
Texas Research Institute, Austin, Texas*

National Aeronautics and
Space Administration

Langley Research Center
Hampton, Virginia 23681-2199

Prepared for Langley Research Center
under Contract NNL07AA00B

February 2009

The use of trademarks or names of manufacturers in this report is for accurate reporting and does not constitute an official endorsement, either expressed or implied, of such products or manufacturers by the National Aeronautics and Space Administration.

Available from:

NASA Center for AeroSpace Information
7115 Standard Drive
Hanover, MD 21076-1320
443-757-5802

CONTENTS

| | Page |
|--------------------------------------------------------------------------|-------------|
| List of Figures | iv |
| List of Tables | vi |
| 1.0 INTRODUCTION | 1 |
| 1.1 Objective | 1 |
| 1.2 Scope | 1 |
| 2.0 BACKGROUND – FRP COMPOSITES | 2 |
| 3.0 NDE FOR MANUFACTURING QUALITY CONTROL | 4 |
| 3.1 Cure Monitoring | 5 |
| 3.2 Porosity | 8 |
| 3.3 Fiber/Matrix Distribution | 13 |
| 3.4 Fiber Volume Fraction | 14 |
| 3.5 Fiber Orientation | 15 |
| 3.6 Fiber Waviness | 19 |
| 4.0 NDE FOR IN-SERVICE DEGRADATION AND DAMAGE | 21 |
| 4.1 Delaminations | 21 |
| 4.2 Impact Damage | 29 |
| 4.3 Heat Damage | 38 |
| 4.4 Stress Rupture | 39 |
| 5.0 STANDARD PRACTICES IN INDUSTRY AND GOVERNMENT | 39 |
| 5.1 Recent Development of Document Standards for NDE of Composites | 39 |
| 5.2 Additional Document Standards for NDE of Composites | 41 |
| 6.0 CONCLUSIONS AND PROGNOSIS | 42 |
| 7.0 REFERENCES | 42 |

List of Figures

| | | Page |
|--------------|-----------------------------------------------------------------------------------------------------------------------------------------------------------------------------------------------------------------------------------------------------------------------|-------------|
| Figure 3.1 | LaserUT system inspecting a complex-contoured composite part | 4 |
| Figure 3.1.1 | Extrusion Fabry-Perot interferometer modified with magnetostrictive actuator coating to measure matrix viscosity..... | 5 |
| Figure 3.1.2 | Plot of tan delta for freshly-mixed Devon “Two-Ton” epoxy, using prototype fiber optic cure monitor | 6 |
| Figure 3.1.3 | The change in ultrasonic sound speed and temperature of an epoxy-graphite fiber prepreg during a compression molding process..... | 6 |
| Figure 3.1.4 | Acoustic waveguide cure curve for part with two right angle bends molded using Shell 815 resin with accelerator and heated via infrared | 7 |
| Figure 3.2.1 | Comparison of ultrasonically determined void content in carbon-epoxy laminates made from unidirectional prepregs with void content determined by acid digestion..... | 9 |
| Figure 3.2.2 | Comparison of Ultrasonically determined void contents in woven carbon-epoxy laminates with those determined by acid digestion | 9 |
| Figure 3.2.3 | Laser ultrasonics setup features a Confocal Fabry-Perot Interferometer and two lasers for generation and detection of surface acoustic waves..... | 10 |
| Figure 3.2.4 | Ultrasonic pulse-echo C-scan (left) of quasi-isotropic thermoset panels shows variations of intentionally introduced void content in the four quadrants. Lock-in IR thermography image (right) of same panel correlates well with the ultrasonic C-scan results | 10 |
| Figure 3.2.5 | Robotic ultrasonic nondestructive workstation..... | 11 |
| Figure 3.2.6 | Two-dimensional waveform histograms for the 0.17% porosity sample (left) and the 3.57% porosity sample (right)..... | 11 |
| Figure 3.2.7 | Schematic of laser optoacoustic evaluation of optically absorbing medium | 12 |
| Figure 3.3.1 | Unenhanced C-scan of 64-ply graphite-epoxy sample (bottom) with matrix-rich areas (center) and matrix-starved areas (top)..... | 14 |
| Figure 3.4.1 | Single-point thermal diffusivity measurement setup | 15 |
| Figure 3.5.1 | In a polar scan, the target spot is impinged at constant distance from all possible angles (θ , ϕ) | 16 |
| Figure 3.5.2 | Schematic representation of the three probes used to detect the fiber orientations in carbon-fiber composites. Each probe consists of a transmitting coil and a receiving coil..... | 17 |
| Figure 3.5.3 | Setup for plate wave flow pattern method | 18 |
| Figure 3.6.1 | Trace maps of rays in 200-ply IM6G/3501-6 unidirectional lamina with wavy fibers | 21 |

| | | Page |
|---------------|----------------------------------------------------------------------------------------------------------------------------------------------------------------------------------------------------------------------------------------------------------------------------------------------------------------------------------------------------------------------------------------------------------------------------------------------------------------------------------------------------------------------|-------------|
| Figure 4.1.1 | Fundamentals of digital shearography: (a) schematic of a typical digital shearography setup using a modified Michelson interferometer as a shearing device; (b) interference phase ϕ before loading; (c) interference phase ϕ' ($=\phi+\Delta$) after loading; (d) the calculated phase distribution ϕ for a square plate clamped all around and loaded centrally; (e) the calculated phase distribution ϕ'' ; (f) the relative phase change obtained by subtracting ϕ from ϕ' | 22 |
| Figure 4.1.2 | Typical shearography set-up | 23 |
| Figure 4.1.3 | Typical ESPI set-up | 23 |
| Figure 4.1.4 | ESPI of a damaged $[\pm 45, 0, 90T]_s$ sample | 24 |
| Figure 4.1.5 | Shearogramme of the same sample as in Figure 4.1.4 | 24 |
| Figure 4.1.6 | Reconstructed displacement field of Figure 4.1.5 | 24 |
| Figure 4.1.7 | Double through-transmission scan of the NPL-designed standard reference panel with 24 reference defects and stepped thicknesses of 5, 4, 3, 2 and 1 | 25 |
| Figure 4.1.8 | Holographic interferometry system layout | 26 |
| Figure 4.1.9 | Variation of $\Delta R/R_0$ in the through-thickness direction with the percentage of fatigue life during tension-tension fatigue for a crossply composite. (a) Minimum $\Delta R/R_0$ at the end of a cycle. (b) Peak $\Delta R/R_0$ in the middle of a cycle | 27 |
| Figure 4.1.10 | Schematic diagram of fiber optic sensor | 28 |
| Figure 4.1.11 | Schematic diagram of sonic-infrared imaging technique | 29 |
| Figure 4.2.1 | Experimental and theoretical phase differences between defective areas and non-defective areas produced by an 11-mm diameter defect at a depth of 0.56 mm | 31 |
| Figure 4.2.2 | Optical configuration of phase stepping ESPI | 33 |
| Figure 4.2.3 | Phase maps of four impacted coupons | 34 |
| Figure 4.2.4 | Damage profiles detected by ultrasonic C-scan | 35 |
| Figure 4.2.5 | Damage profile of impacted coupons by sectioning technique | 36 |
| Figure 4.3.1 | Block diagram of the thermo-elastic material characterization experimental set-up | 38 |

List of Tables

| | Page |
|------------------------------------------------------------------------------------------------------------------------------------------|-------------|
| Table 3.5.1 Specific conductivity of metals and CFRP | 17 |
| Table 4.2.1 Comparison of damage areas determined by intensity fringes, phase maps, ultrasonic C-scan and sectioning techniques | 36 |
| Table 4.2.2 Defect size for the NDT techniques..... | 37 |

1.0 INTRODUCTION

1.1 Objective

Advanced fiber reinforced polymer composite materials continue to be used in a large number of applications ranging from aerospace to automotive, industrial and consumer products. The high stiffness-to-weight ratio, low electromagnetic reflectance, and the ability to embed sensors and actuators have made advanced fiber reinforced composites an attractive alternative construction material for primary aircraft structures. In many other cases fiber reinforced polymer composite materials are being developed and used to replace metal components, in particular in corrosive environments.

The advantages of advanced composite materials in modern structures are well known: strength, stiffness, lightweight, and corrosion resistance. Typical aerospace applications for advanced composites are ultra-high-performance pressure vessels, rocket motor cases, and launch tubes. Aeronautical applications include helicopter rotor blades, external fuel tanks for combat aircraft, and more recently composite fuselages. Commercial applications cover a wide range of uses including bike frames, tennis rackets, fuel containers used to store compressed natural gas for motor vehicles, and high-performance tubular products used in the offshore oil and gas industry.

Because of their increasing utilization in structural applications, the nondestructive evaluation (NDE) of advanced fiber reinforced polymer composites continues to receive considerable research and development attention. Due to the heterogeneous nature of composites, the form of defects is often very different from a metal and fracture mechanisms are more complex. The purpose of this report is to provide an overview and technology assessment of the current state-of-the-art with respect to NDE of advanced fiber reinforced polymer composites.

1.2 Scope

Advanced fiber reinforced polymer composites generally require unusual processing operations in order to achieve their unique microstructures and geometry. Rejection rates in the manufacture of these materials tends to be higher than that for more conventional materials, and the unpredictable variability of properties prevents the designer from utilizing these materials to their full potential. In order to achieve better process control in the manufacture of both advanced and conventional materials, a new paradigm of intelligent processing of materials started to emerge in the second half of the 1980's. Because of the importance of manufacturing quality control for advanced fiber reinforced polymer composites Section 3.0 of this assessment reviews NDE research and development that has focused on improving the manufactured quality of composites, and covers composite characteristics important to processing including: cure, porosity, fiber/matrix distribution, fiber volume fraction, fiber orientation and fiber waviness.

Section 4.0 reviews research and development that has focused on NDE for detection and characterization of in-service damage and degradation. Topics covered include impact damage, delaminations, disbonds, heat damage and importantly, stress rupture degradation.

Section 5.0 provides information on document standards for the inspection and NDE of advanced fiber reinforced composites. It should be noted, that in contrast to the large numbers of NDE document standards available for the inspection of metals, there are a very limited number of document standards available for NDE of composites. To help alleviate this situation, in late 2004, NASA helped initiate an effort to develop national consensus document standards for NDE of aerospace composites. This effort has resulted in the recent development of six ASTM International document standards: a standard guide for NDE of aerospace composites and standard practices for acoustic emission, ultrasonics, shearography,

thermography and radiography. Information is provided in this section on the current status of this effort and includes information on other document standards for NDE of advanced fiber reinforced polymer composites for use by industry and the government.

Conclusions and prognosis regarding NDE of advanced fiber reinforced polymer composites is presented in Section 6.0 and references are provided in Section 7.0.

In compiling this technology assessment, literature searches were conducted in the NTIAC data base (the world's largest NDE data base) commercial scientific and engineering data base, and a web based scientific data base. The searches were confined to the years 2001 to the present in order to supplement and upgrade the NTIAC Technology Assessment on NDE of Fiber Reinforced Composite published in July 2001. Upon examination of the lengthy literature search results, forty-four papers were determined to be relevant to the current technology assessment and were acquired for review. Information was also collected on standard practices used by government agencies and the aerospace industry for NDE of fiber reinforced composites.

2.0 BACKGROUND-FRP COMPOSITES

Advanced materials, such as modern polymer matrix composites, are capable of providing outstanding or specialized properties, or combinations of properties, that cannot be obtained in conventional materials. The unique properties of advanced materials are the result of the sophisticated microstructure that is designed and built into the material. Polymer matrix composites also provide unique properties due to their synergistic combination of high-performance fibers and matrices. The fiber provides the high strength and modulus, and the matrix spreads the load and provides protection from weathering and corrosion.

A fundamental reason for the popularity of advanced composite materials is the flexibility that is presented to a designer in tailoring the material properties to the application. This is achieved by selection of the resin matrix, fiber reinforcement and fiber geometry to yield the desired response in the finished component or structure.

Composite materials are formed by combining two or more materials that have quite different properties, so that the different materials work together to give the composite its unique properties. In general, composite materials are very durable; the right composites stand up well to heat, corrosion, and cyclic loading. Another advantage of composite materials is that they can be molded into complex shapes, and designers can reduce the number of small parts in a system by combining several small parts into one larger composite component. The disadvantages of advanced composites are the cost, the manufacturing processes tend to be complex, and the nondestructive evaluation of parts during and after manufacture or in-service is often more difficult than with conventional homogenous metals, polymers, and ceramics.

Glass fibers, by far the most common reinforcement, are made of silicon oxide with the addition of small amounts of other oxides. These fibers generally have high tensile strength, good temperature and corrosion resistance, and low price. However, the glass fibers are also brittle and will break if bent sharply. Glass fibers are used as reinforcing materials in many composite applications; for example car bodies and panels, boat hulls, swimming pool liners and surf boards.

Carbon fibers are the stiffest and strongest reinforcing fibers for polymer composites, and, after glass fibers, are the most used. Made of pure carbon in the form of graphite, these fibers have low density and a negative coefficient of longitudinal thermal expansion. However, the drawbacks are that carbon fibers are very expensive and can produce galvanic corrosion when in contact with metals. Carbon fibers are generally used with epoxy, where high strength and stiffness are required. Carbon fiber reinforced

polymer composites find uses in, for example, racecars, automotive, aeronautical, aerospace, and medical applications (to repair or replace damaged bones), and sports equipment. Hybrid blends of glass and carbon fibers are also used to enhance mechanical properties without occurring the high cost of using only carbon fibers.

Epoxy is a strong and very resistant thermoset polymer. Curing of the epoxy takes place by adding a hardening agent and sometimes applying heat. The type of hardener used has a major influence on the properties and applications of epoxies. Epoxy is resistant to almost all acids and solvents, but not to strong bases or solvents with chlorine content. It is used as an adhesive agent, as filling material, for molding dies, and as a protective coating on steel and concrete. Many polymer composite materials have an epoxy matrix.

Composite materials represent acoustically and thermally heterogeneous materials where a variety of defects with different dimensions may be formed. Typical defects of composite materials include fiber breaks, microcracks, microsplits, foreign objects, and pores in the bonding medium, and detachment of fibers from the bonding material. Fiber waviness, fiber orientation and fiber/volume fraction are also important microstructural properties of composites. Many of these defects or microstructural variations result in changes of the acoustic attenuation and the speed of sound in composite materials. That is why ultrasonic NDE is currently one of the most frequently used methods for inspection of polymer matrix composites. Many of these defects and microstructural changes also result in changes in the thermal properties of the material and so thermography is also often used to inspect polymer composites.

Composite materials must be regarded as very different media from metals, when considering which NDE methods are appropriate. Generally the reinforced plastics have poor electrical conductivity, low thermal conductivity, high acoustic attenuation and significant anisotropy of the mechanical and physical properties. The life of a metal component is determined by the nucleation and growth of cracks or damage in the material. The development of linear elastic fracture mechanics is often adequate as a basis for the definition of the size of subcritical flaws (referred to as NDE accept/reject criteria set by the designer), which must be identified.

However, a fiber reinforced plastic is a heterogeneous medium that can contain multiple defect geometry's. No single failure model can adequately describe the level of damage that is critical. A multiplicity of models has been developed to describe the various failure possibilities: interlaminar debonding, matrix degradation, fiber fracture, and fiber matrix separation. These in turn may be caused by improper cure, fiber misalignment, inclusions, poor reinforcement distribution, machining damage, fastener fretting, fatigue, impact damage, heat damage, stress rupture and environmental degradation.

The ever-increasing demand for higher quality composite materials has driven engineers to improve manufacturing processes and inspection of the product. For some manufacturing methods, in-process inspection may provide a means to improve quality and efficiency. Continuous composite manufacturing processes, such as pultrusion, are ideal candidates for in-process inspection. In a continuous process, the consolidated composite passes a common location at a particular point in the manufacturing cycle. A nondestructive evaluation station placed at that location would thus have the capability of 100% inspection of the finished product.

In-situ NDE must be done quickly to keep up with the manufacturing process. Thus, in this situation, a quick measurement of bulk ultrasonic properties is preferable to measuring the same property at each point on the sample and building up an image based on the individual responses as in ultrasonic C-scan testing. Attenuation, and longitudinal and shear wave velocities all provide for measurements of bulk materials properties and have been used to measure porosity in various composite materials.

3.0 NDE FOR MANUFACTURING QUALITY CONTROL

This section reviews NDE research and development that has been focused on improving the manufactured quality of composites, and covers composite characteristics important to processing including: cure, porosity, fiber/matrix distribution, fiber volume fraction, fiber orientation, and fiber waviness. Delamination is another important flaw that can occur during composite processing, but NDE of delaminations will be covered later in this review in Section 4.1.

The processes used in manufacturing advanced composites include:

- Hand Lay-up of the part with computer software to keep track of the materials and process.
- Automated Tape Lay-up of the part where machines generally are used to make large, mildly contoured parts.
- Ply Cutting and Stacking to support the hand lay-up process where reciprocating knives, ultrasonic, lasers and high-pressure water are used to cut the plies.
- Filament Winding is used more often than all other processing techniques. It is well suited to pressure vessels and involves a spindle with one or more carriages to apply hoop and helical fibers.
- Tow Placement is a combination of filament winding and tape laying.
- Pultrusion is one of the few continuous composite fabrication processes that can be used to lower cost, but it produces mostly low technology composites.
- Liquid composite molding (LCM) includes Resin Transfer Molding (RTM), structural reaction injection molding (SRIM), and injection compression molding (ICM). A fiber preform is placed in the mold cavity and polymer resin is injected into the closed mold. After solidification, the part is removed from the mold. Since the tooling costs are high, it is most attractive for high production run parts.
- Curing of thermoset polymer matrix composites is carried out in autoclaves, ovens and microwave ovens.
- Thermoforming is carried out with thermoplastic matrix composites and they are liquid at processing temperatures.

It is interesting to note that Voillaume, et al. (2006) analyzed the applications of automated robotic, laser ultrasonics to composite manufacturing for commercial aircraft. The authors focused their study on the LaserUT equipment developed, and used by Lockheed Martin Aeronautics. Figure 3.1 shows the LaserUT system inspecting a complex-contoured composite part.

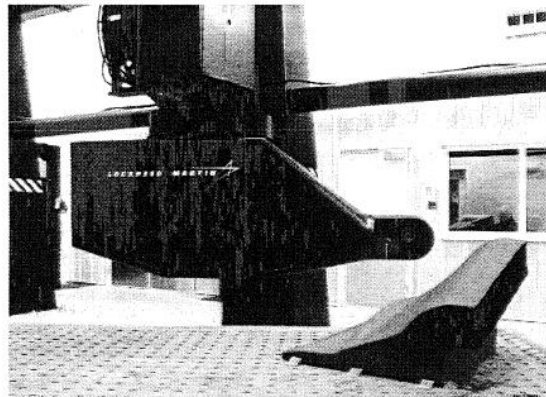


Figure 3.1. LaserUT system inspecting a complex-contoured composite part.

The authors concluded that the LaserUT system will save several hundred million dollars in lower capital and labor costs compared to other ultrasonic inspection technologies over the life of the F-22 and F-35 fighter programs alone. These huge savings are due to the type of parts found on fighters that are relatively small and highly contoured. The authors believe that future LaserUT systems with kHz scanning speeds will seriously challenge dedicated conventional multi-channel ultrasonic systems even for the inspection of large and less-complex parts on commercial aircraft. An in-service Laser UT system demonstration on an aircraft is scheduled for 2010, and EADS CCR/Airbus is currently investigating the use of LaserUT for on-line monitoring of composite manufacturing processes.

3.1 Cure Monitoring

The quality of thermoset polymer matrix composites is heavily dependent on the curing cycle, which is in turn dependent on the rate of the speed of the temperature increase, the temperature of the curing plateau, the time at which pressure is applied, and the post curing temperature and pressure. In order to achieve high quality, the cure cycle must be optimized before actual production is undertaken.

May and Claus (1996) used a fiber optic strain sensor coupled to a miniature actuator as an in-situ cure monitor for thermoset polymer composites. The miniature actuator can be made to vibrate while immersed in a curing resin. Comparison of the phase of the electrical actuation to the phase of the resulting strain in the sensor permits a measure of the loss tangent of the resin, where the loss tangent is the ratio of the loss modulus to the storage modulus.

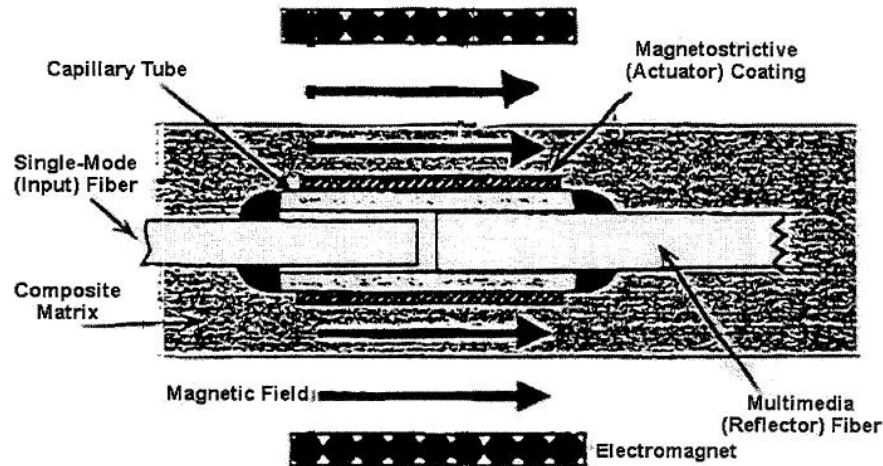


Figure 3.1.1. Extrusion Fabry-Perot interferometer modified with magnetostrictive actuator coating to measure matrix viscosity. May and Claus (1996)

As the crosslinking of the resin proceeds, the loss tangent also changes, reflecting the changing rheology of the resin. The loss tangent is at maximum at the gel point of the resin, and further crosslinking may be tracked as the loss tangent decreases following gelation. After the part is completely cured, the fiber optic sensor can function as an in-service strain sensor. Figure 3.1.1 illustrates the conceptual design of the sensor, and Figure 3.1.2 shows that the sensor has captured the main features of the behavior due to changing viscoelasticity of the resin.

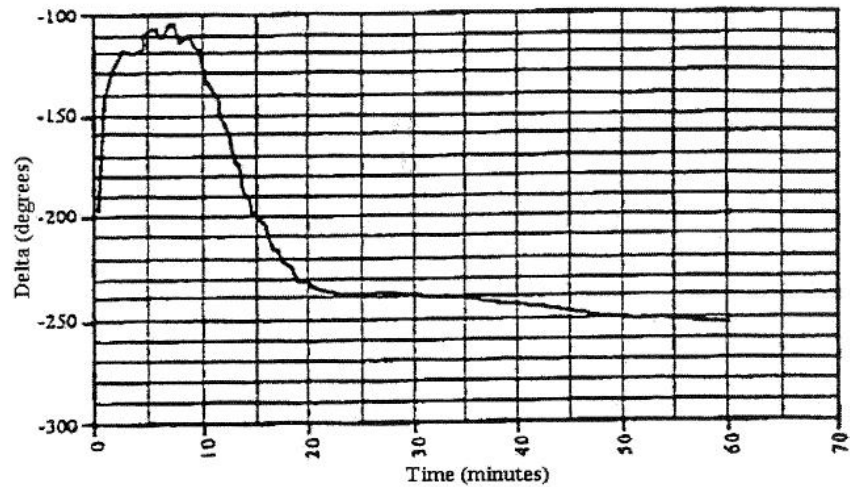


Figure 3.1.2. Plot of tan delta for freshly-mixed Devcon "Two-Ton" epoxy, using prototype fiber optic cure monitor. May and Claus (1996)

Ultrasonics has also been extensively investigated for its applicability to on-line process control. Kline, et al. (1994) used high temperature piezoelectric transducers to monitor the cure cycle of polymer matrix composites at high temperatures in an autoclave. They measured the amplitude and velocity of longitudinal and shear waves during the cure cycle, and they were able to determine resin viscosity changes, the efficiency of the part consolidation process, and then cross-link formation in the matrix.

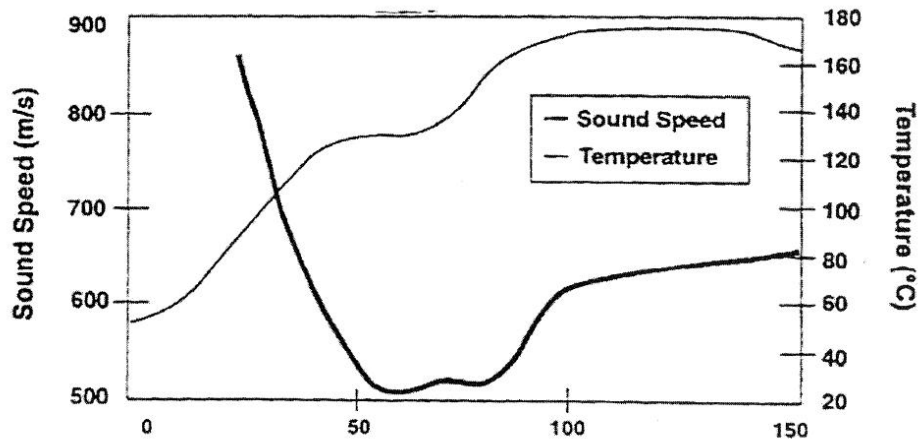


Figure 3.1.3. The change in ultrasonic sound speed and temperature of an epoxy-graphite fiber prepreg during a compression molding process. Shepard and Smith (1996)

In addition, Shepard and Smith (1996) have developed a commercially available ultrasonic system for in process monitoring and control of the cure at temperatures up to 260°C in molds. Figure 3.1.3 shows the change in sound speed of an epoxy-fiber prepreg during a compression molding process. The initial decrease in sound speed shows the decrease in viscosity as the prepreg increases in temperature. A broad minimum is shown as the temperature cycle enters a 121°C hold period, and is followed by an increase in sound speed as the temperature is increased to 177°C. The rate of increase in the sound speed then slows as the rate of cure slows and the reaction nears completion. They were also able to obtain a good correlation between ultrasonic measurement results and those obtained simultaneously with dielectric

measurements that have been shown to correlate well with viscosity and cure state in thermosetting composites.

Biermann, et al. (1996) also demonstrated an ultrasonic sensor approach to monitoring graphite/epoxy composite curing in an autoclave and were able to follow changes in viscosity and determine end-of-cure.

Embedded acoustic sensors have been used to remotely monitor the state of cure, viscosity, and modulus of resin during the cure cycle. Embedded acoustic wave-guides of 0.25-mm diameter Nichrome® wire were used by Harrold, et al. (1994) to monitor the real time curing of composites. They were able to correlate the ultrasonic wave attenuation data with viscosity, gelation and modulus of the resin. In addition, they pointed out that the embedded sensors, using acoustic wave velocity, were also able to monitor internal residual strain and material modulus after the part is manufactured. After the part is placed in service, the embedded sensors can also monitor for damage and remaining life. The authors used frequencies in the range of 60 to 80 kHz and were able to monitor parts that had right-angle bends.

In order to understand how the acoustic wave-guide works, it is instructive to look at the acoustic impedance of the system. The acoustic impedance of a material is equal to the density times the acoustic wave velocity. If the acoustic impedance of the host material matches that of the acoustics wave-guide, then only a small amount of ultrasonic signal will be transmitted in the wave-guide as most of the signal is attenuated. However, if the acoustic impedance of the host material is different than that of the wave-guide, then reflections at the interface will allow a larger ultrasonic intensity to be transmitted in the wave-guide and there is less attenuation. Therefore, during the processing of a thermoset polymer composite, the changes from a liquid to a highly viscous solution, to a rubber gel, to a more rigid material, and finally to a high modulus state can be traced by changes in the attenuation of the ultrasonic signal in the wave-guide. Typical embedded acoustic wave-guide cure curves of signal level and wave velocity for an epoxy resin are shown in Figure 3.1.4.

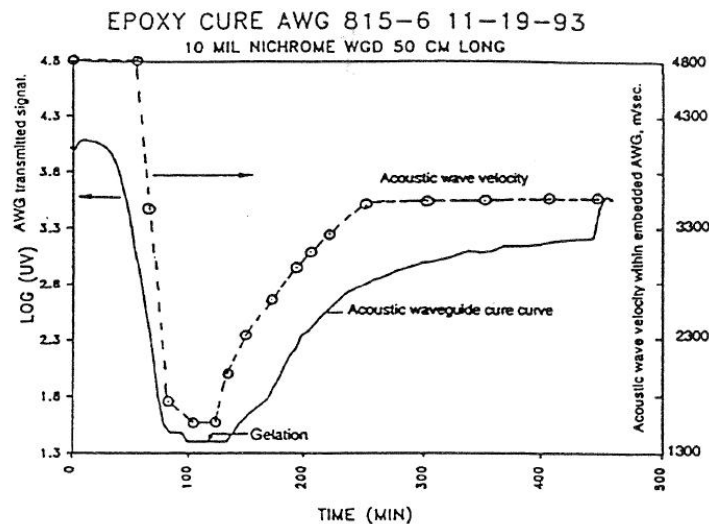


Figure 3.1.4. Acoustic waveguide cure curve for part with two right angle bends molded using Shell 815 resin with accelerator and heated via infrared. (Harrold 1994)

Dielectric measurements have also been used for cure monitoring of thermoset polymer matrix composites using embedded electrodes. The dielectric properties of resin during curing vary over a very large range as the resin cures. Commercial equipment is available to monitor dielectric properties of

curing resin that use prefabricated electrodes. This dielectric monitoring technique is based on early work by both Sentra and Shepard (1995) and Rice and Lee (1996).

3.2 **Porosity**

Porosity, in the form of distributed voids, is a perennial problem in composite manufacturing, especially for laminated structures such as carbon-fiber-reinforced polymer composites. Porosity in composites may be the result of a number of conditions including:

- Uneven wetting of the fibers
- Incomplete chemical reactions
- Inappropriate chemical reactions
- Degassing of contaminants (e.g., oils and silicones)
- Improper or incomplete debulking leaving air trapped between the plies
- Poor ventilation restricting the removal of any out gassing of the panel.

No matter what the source, porosity can have a detrimental effect on the performance of the structure by leaving regions of unsupported fibers and points of stress concentration. An increase in porosity leads to a decrease in density, modulus, and strength of a composite. Determining levels of porosity is an important practical issue and void content is often regarded as a measure of quality by the composites industry. In composites, the voids can be within the matrix, between plies, or at the fiber/matrix interface.

Ultrasonic NDE techniques for determining porosity in composites may be broadly categorized as either direct ultrasonic imaging, correlation with a single ultrasonic frequency (narrowband approach), or correlation with ultrasonic frequency slope (broadband approach).

Direct ultrasonic imaging of the porosity may be useful if the pore size is sufficiently large (greater than the resolution cell size of the ultrasonic image). However, this technique may require additional image processing and can be difficult to quantify.

Of the two empirical techniques, correlation of the frequency slope of the attenuation curve has been successfully demonstrated and widely applied. In work by Hsu (1988) the author used through-transmission ultrasonics to determine void content (volume percent) of a carbon-fiber-reinforced plastic (CFRP). The void content is directly proportional to the slope of the attenuation with respect to frequency, also known as the attenuation slope. The author obtained the frequency dependent attenuation in the 2 to 16 MHz range on carbon-epoxy and carbon-polyimide composites containing up to 12 % voids in woven laminates and up to 6 % voids in nonwoven unidirectional and quasi-isotropic laminates. Figure 3.2.1 shows the results for nonwoven laminates and Figure 3.2.2 shows the results for woven laminates.

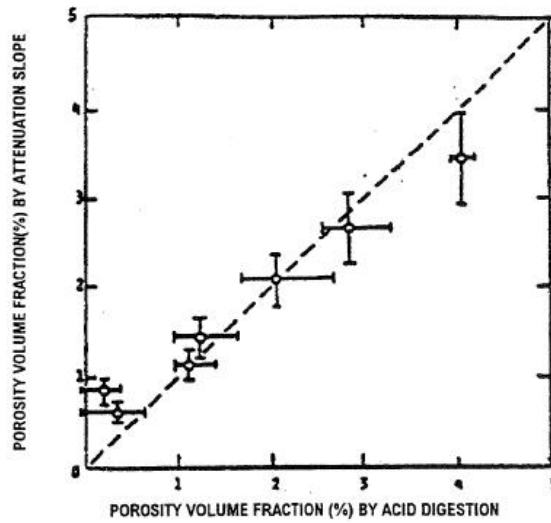


Figure 3.2.1. Comparison of ultrasonically determined void content in carbon-epoxy laminates made from unidirectional preregs with void content determined by acid digestion. (Hsu 1988)

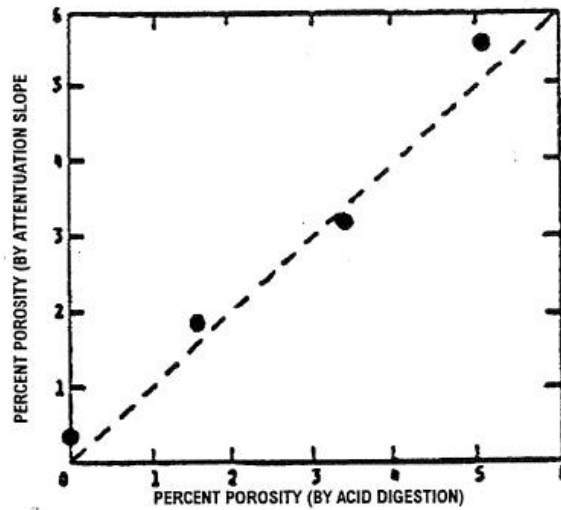


Figure 3.2.2. Comparison of ultrasonically determined void contents in woven carbon-epoxy laminates with those determined by acid digestion. (Hsu 1988)

Thermography and laser based ultrasonics to determine porosity in thermoplastic composite fabrication have been investigated by Steiner (1996). Figure 3.2.3 shows a Schematic of their laser based equipment set up and Figure 3.2.4 shows both their laser-based results and their results using lock-in thermography.

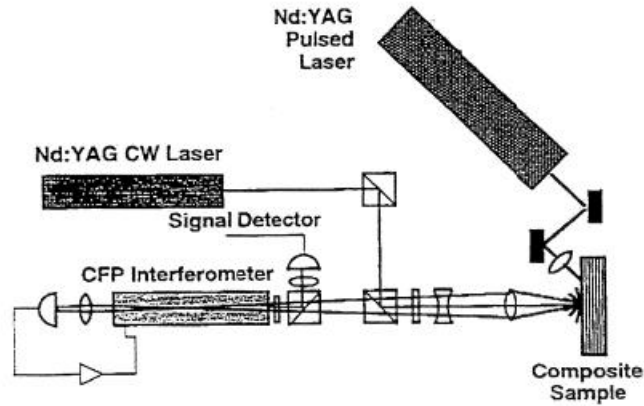


Figure 3.2.3. Laser ultrasonics setup features a Confocal Fabry-Perot Interferometer and two lasers for generation and detection of surface acoustic waves. (Steiner, et al. 1996)

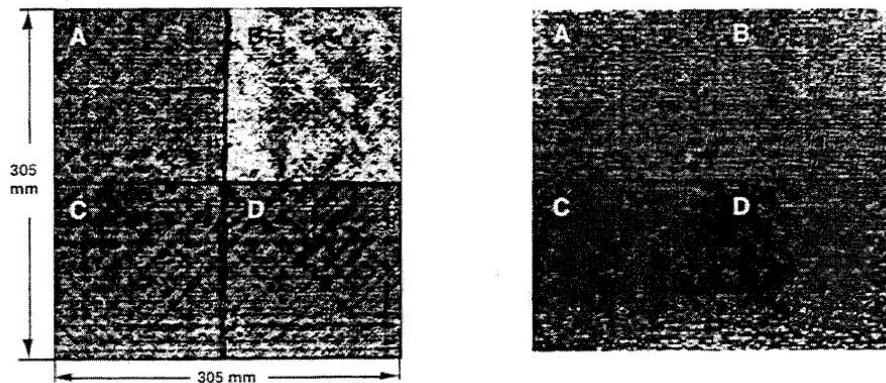


Figure 3.2.4. Ultrasonic pulse-echo C-scan (left) of quasi-isotropic thermoset panels shows variations of intentionally introduced void content in the four quadrants. Lock-in IR thermography image (right) of same panel correlates well with the ultrasonic C-scan results. (Steiner, et al. 1996)

In order to determine the amount of porosity, Steiner (1992), in an earlier study than the one described above, used ultrasonic pulse-echo C-scan imaging to study composite panels with various porosity contents. The samples ranged from 1.17% to 3.57% porosity and had a thickness of about 2-mm. A 15-MHz transducer with a scan increment of 0.23 mm was chosen for use on a robotic ultrasonic inspection system (see Figure 3.2.5). The ultrasonic receiver gain was selected such that none of the resulting C-scan images (histograms) were either over- or under-saturated. Subsections of the porosity panels were subjected to digitized full-volume waveform analysis. A useful feature of the full-waveform analysis program is the ability to produce two-dimensional waveform histograms. Superimposing all individually digitized waveforms generates these histograms. The resulting image gives a clear indication of the waveform distribution and of occurring abnormalities. Figure 3.2.6 compares two 2-dimensional waveform histograms relating to a sample with low porosity (0.17%) and a sample with high porosity (3.57%). The low-porosity sample shows almost no echo activity between the front and the back echo, whereas the high-porosity sample features a dramatic increase in echo activity between front and back echoes, thus reducing the back echo.

This technique demonstrates the influence of voids on the ultrasonic waveform. These porosity studies were directed towards qualitative rather than quantitative results. In order to use ultrasonic NDE techniques to measure the porosity contents, it will be necessary to establish a database by preparing and measuring an appropriate number of samples with known void contents and then to relate future scan data to the established database Steiner (1992).

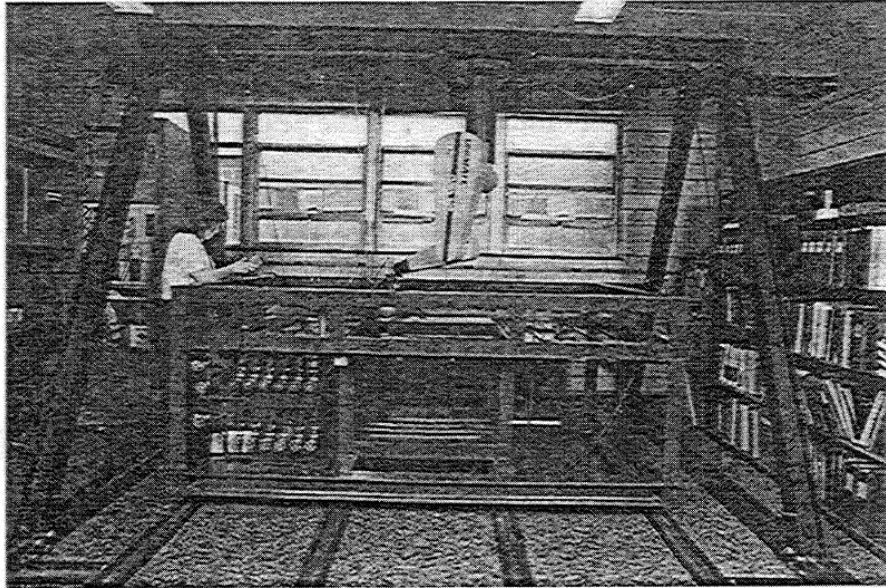


Figure 3.2.5. Robotic ultrasonic nondestructive workstation (Steiner 1992).

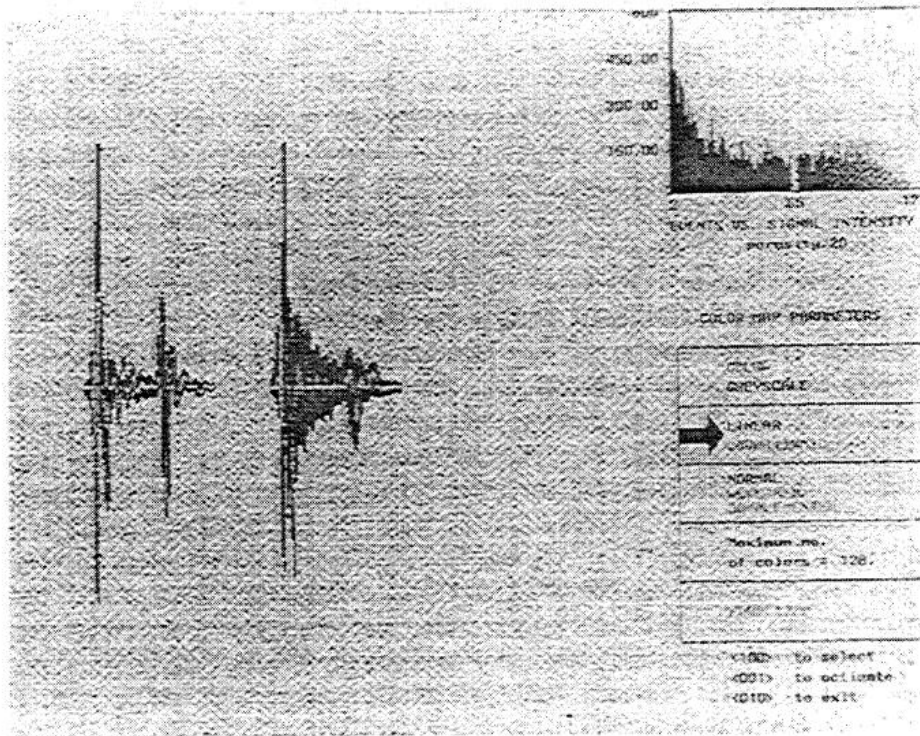


Figure 3.2.6. Two-dimensional waveform histograms for the 0.17% porosity sample (left) and the 3.57% porosity sample (right). (Steiner 1992)

Karabutov et al. concluded that laser optoacoustic monitoring might be a method for nondestructive evaluation of the porosity of composite materials, particularly if only one surface is accessible. Furthermore, they believe that a quantitative analysis of the temporal profiles of the backscattered wide-band ultrasonic signals may yield novel quantitative characteristics for graphite composites: a cross section of ultrasound backscattering. A laser optoacoustic sensor was shown to be capable of detecting structural heterogeneities and may potentially reveal the nature of defects, such as porosity or layer separations. And because this technique uses a laser to excite the test object, a couplant is not required, allowing it to be used on in-service structures.

McRae and Zala (1995) characterized the linear variation of attenuation with frequency using the constant-Q model, a model previously developed for use in seismic applications. This method requires only that the acoustic impedances of the system are known and that the surface and interface reflections are resolvable. The accuracy of the method was verified in tests with synthetic data. Values of Q were then estimated for each of a series of six graphite-epoxy laminate specimens with known porosities in the region of 0.34% to 5.33%. These specimens were about 0.29-cm thick and were scanned on a 128-by-128-element grid (2.6 cm on a side); 256-element traces were collected using a broadband 5-MHz focused transducer and sampling rate of 50 MHz. The measurements showed a strong inverse correlation between Q and porosity, and suggest that Q may provide a sensitive and quantitative means of estimating porosity, especially for the critical region of low porosity levels.

It should be noted that in a review of NDE methods for porosity measurement in fiber reinforced polymer composites by Brit and Smith (2004), the authors stated that none of the current NDE techniques (ultrasonics, thermography, and microwave) are ready for in-service inspection since there is a dependence on pore morphology and the fiber and resin matrix materials. However, the authors of this current technology assessment (Yolken and Matzkanin) believe, that in a well controlled process development or production environment, pore morphology and the materials are mostly controlled or known, and that ultrasonic methods can yield quantitative porosity information. Results will be dependent on geometry, physical calibration standards with similar geometry and materials being used by well-trained inspectors to alleviate this problem.

3.3 Fiber/Matrix Distribution

The distribution of fibers and matrix (matrix distribution) is critical to the performance of a composite structure. Knowledge of the size and location of matrix-rich pockets and matrix-starved regions provides important information that can be used in finite element codes to calculate performance influences. Little work has been reported in the literature on this NDE problem. However, Steiner (1992) used ultrasonic pulse-echo C-scan imaging to evaluate a 64-ply graphite-epoxy composite sample. The fibers and the matrix react differently to ultrasonic energy. While the fibers reflect the energy, the matrix tends to absorb the energy. Although the differences may be subtle, image-enhancing techniques aid in the determination of matrix-rich or matrix-starved areas in the scanned specimen. Figure 3.3.1 shows the specimen with matrix-rich areas in the center and matrix-starved area at the top.

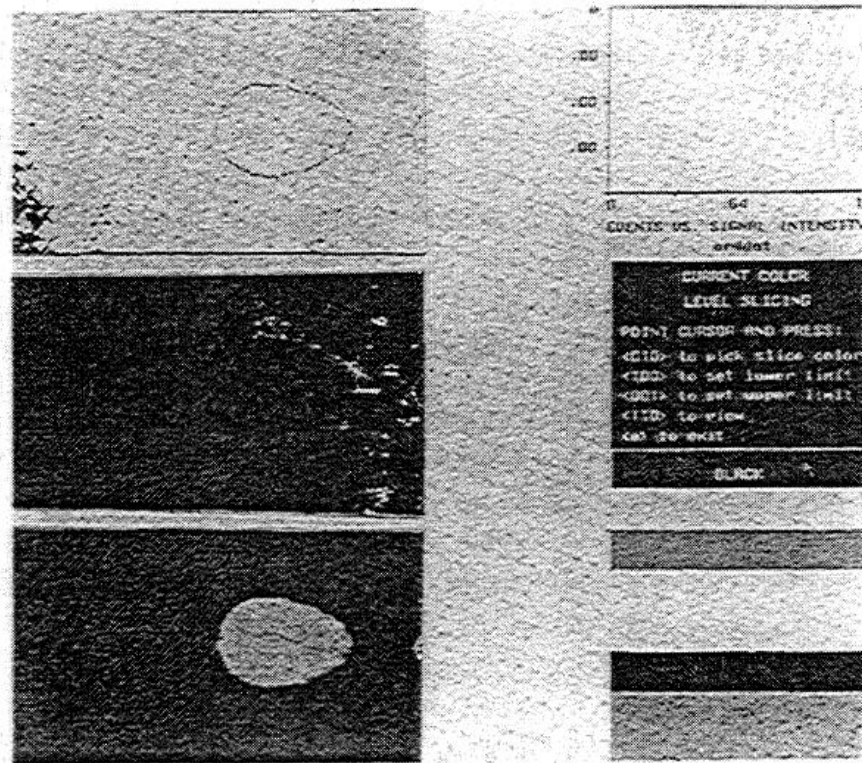


Figure 3.3.1. Unenhanced C-scan of 64-ply graphite-epoxy sample (bottom) with matrix-rich areas (center) and matrix-starved areas (top). (Steiner 1992)

The matrix rich areas are located on the less than average echo intensity side of the pulse-echo histogram, and the matrix-starved regions are located on the higher than average intensity side of the histogram. The sample was sectioned to confirm the ultrasonic results, and an analysis of the manufacturing process showed that autoclave bagging was the primary reason for the variations.

3.4 Fiber Volume Fraction

A composite's strength is determined largely by the interaction between the fiber and the matrix. Since the matrix distributes the load onto and between the fibers, it is important to know the respective volume amounts (volume fraction).

Seale, et al. (1998) studied the determination of volume fraction in composites using ultrasonic Lamb waves. Fiber volume fraction variations in the range of approximately 0.40 – 0.70 were studied and the results were compared to acid digestion. The authors also developed and evaluated a model to predict the fiber volume fraction from Lamb wave velocity values.

Zamaleda and Winfree (1993) and Zamaleda and Smith (1994) investigated a through-transmission, thermal diffusivity measurement technique to determine fiber volume fraction in graphite composite plates. In these studies, the thermal diffusivity was determined and used to characterize the fiber volume fraction in the graphite composite plates, assuming negligible porosity levels. Their results showed that the fiber volume fraction determined for the thermal diffusivity results were typically slightly higher than the destructive test results. The authors said this could be due to the matrix thermal conductivity being

slightly higher than the value found in the literature, and also do to not taken porosity into account in their model.

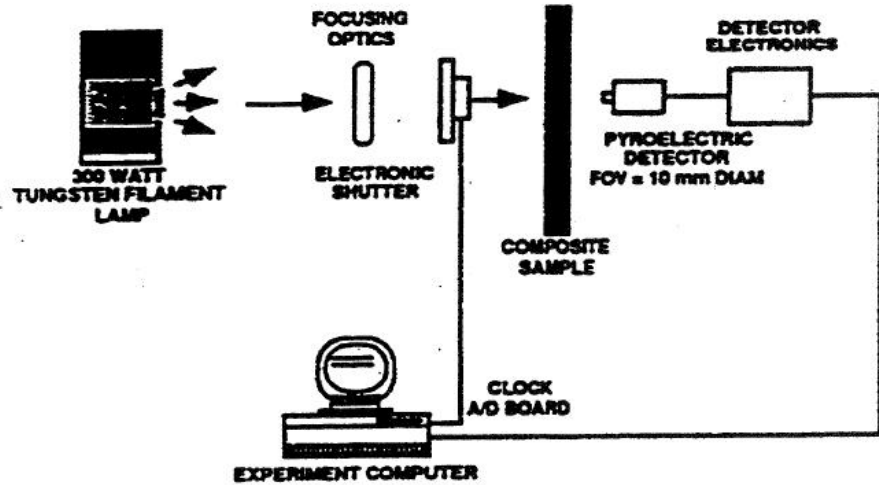


Figure 3.4.1. Single-point thermal diffusivity measurement setup.
(Zalameda and Winfree 1993)

An investigation by Dorsey, et al. (2004) showed that fiber volume fraction in carbon fiber polymer matrix composites can be nondestructively measured by using cold neutron prompt gamma activation analysis (PGGA). PGGA is a technique that can nondestructively determine isotopic and elemental content in materials. It should be noted that PGGA is not a field or usual laboratory technique since it requires a very intense source of cold neutrons that are only available in a few major research establishments. Since this is the case, PGGA should be viewed as a reference NDE technique that is costly and time consuming.

Fiber volume fraction determination is done with PGGA by measuring and comparing the carbon and hydrogen content in a give sample. The authors compared their PGGA results to the gold standard determination of fiber volume fraction, which is a destructive acid digestion test, and the comparison was in good agreement. Fiber volume fraction measurements using PGGA can potentially be applied to any composite where the contents of the matrix and the reinforcement differ. The technique is also spatially sensitive, with the resolution limited by the dimensions of the neutron beam.

3.5 Fiber Orientation

In continuous fiber reinforced polymer matrix composites, the fiber orientation needs to be carefully controlled. This is the case since a small variation of only 10 degrees in the ply orientation can result in a decrease in the stiffness of a composite laminate by about 30 %. Degrieck, et al. (2003) used ultrasonic polar scans at nominally 5 MHz to nondestructively determine the fiber orientation of carbon fiber polymer matrix composites. The polar scan technique utilizes the amplitude of the transmitted (or if necessary reflected) ultrasonic signal. The amplitude is very easy to measure from sound impinging the plate from every direction above the plate. Figure 3.5.1 shows a schematic of an ultrasonic polar scan where the amplitude of the transmitted beam is determined over many angles. The authors also showed that their polar scan technique is also useful in determining fiber volume fraction and porosity in composites.

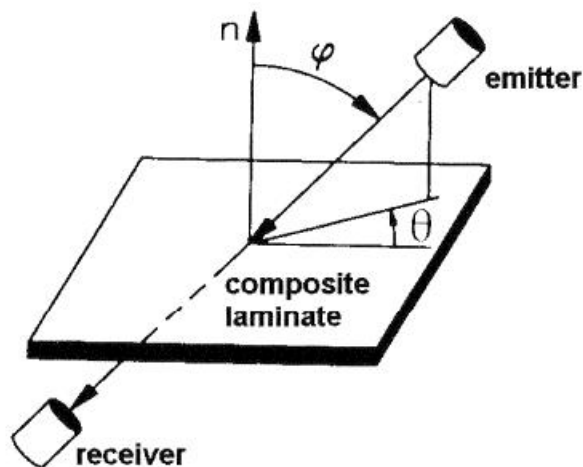


Figure 3.5.1. In a polar scan, the target spot is impinged at constant distance from all possible angles (θ, φ) (Degrieck, et al. 2003)

In an investigation by Fei and Hsu (1999), two motorized PC-controlled ultrasonic azimuthal scanners were used to determine the fiber orientation on graphite epoxy laminates. One scanner was used in a transducer contact mode in the acousto-ultrasonic configuration, and the second scanner was used for EMAT-generated shear wave transmission. The authors were able to obtain good agreement on graphite epoxy laminate between the models they were developing and their experimental results.

A number of other investigators have studied ultrasonic methods for the determination of fiber orientation. For example, Mol (1992) developed a method for automated determination of the fiber orientation by image processing of the ultrasonic C-scan images. The samples were made from CFRP material with a ply thickness of 0.181 mm. Pulse echo scans were made by digitizing each A-scan and by selecting a number of samples with a pre-chosen delay relative to the front surface. Fiber orientation was visually detected in the C-scans to a depth of about 12 plies. Fiber orientation estimation from pulse-echo images for individual plies was successful over a depth of 16 plies. The determination of fiber orientation was correct for plies 3 to 16 (0.24 to 2.6 mm deep) and failed on one or more times down to ply 22. When measuring deeper than ply 22 the signal-to-noise ratio was too low and all information on fiber orientation was lost.

De Goeje and Wapenaar (1992) investigated the possibilities and limitations of eddy current methods for inspecting CRFP composites. In contrast to metals, CRFP composites show inhomogeneous and anisotropic electrical properties as shown in Table 3.5.1. Moreover, the conductivity is much lower than that of metals. For unidirectional composites the conductivity in the fiber direction is a factor of about 1,000 lower than that of metals, while the conductivity in the cross direction is a further factor of about 100 lower. Eddy current methods can only be applied to materials that have high electrical conductivity.

Table 3.5.1. Specific conductivity of metals and CFRP. (de Goeje and Wapenaar 1992)

| Material | Conductivity (10 ⁴ S/m) | Direction of Measurement |
|------------------|------------------------------------|--------------------------|
| Copper | 5900 | |
| Aluminum | 3500 | |
| Iron | 1000 | |
| Graphite | 13 | |
| Carbon | 3 | |
| Carbon fiber | 4-17 | |
| Unidirectional | 0.9-1.5 | Parallel |
| CFRP | 0.01-0.2 | Perpendicular |
| | 2 | Parallel |
| | 0.01 | Perpendicular |
| | 0.13 | Parallel |
| | 0.03 | Perpendicular |
| | 3.6 | Parallel |
| Satin weave CFRP | 0.1-1 | |

The authors tested unidirectional and satin weave carbon fiber/epoxy prepregs, and probes with elliptical coils shown in Figure 3.5.2 were used to determine fiber orientation in the samples. This was done by rotating the probes over 360 degrees while the amplitude of the signal induced in the detector coil was monitored.

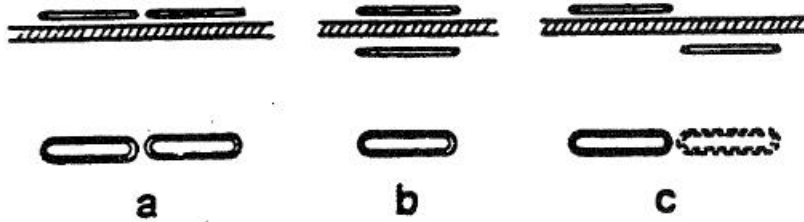


Figure 3.5.2. Schematic representation of the three probes used to detect the fiber orientations in carbon-fiber composites. Each probe consists of a transmitting coil and a receiving coil. (de Goeje and Wapenaar 1992)

Sullivan et al. (1996) conducted an experiment to study ultrasonic plate wave (also called Lamb wave) flow patterns in anisotropic and multi-layered composite materials. Fiberite HYe 1034C prepreg unidirectional tape was used to fabricate all test specimens. All but three of the specimens were 20 plies thick. In the test setup, one transducer transmitted the ultrasonic wave into the specimen while the receiving transducer captured the leaky plate waves that emanate from the top surface of the laminate (see Figure 3.5.3). The transmitter was fixed such that the transmitting probe insonified the test piece at one end, while the receiving transducer scanned the laminate. Both transducers were maintained at the same height from the laminates, and a 10° angle of incidence was used for both transducers. Plate waves were generated to image the flow patterns of ultrasonic waves in multiple laminates of various fiber directions.

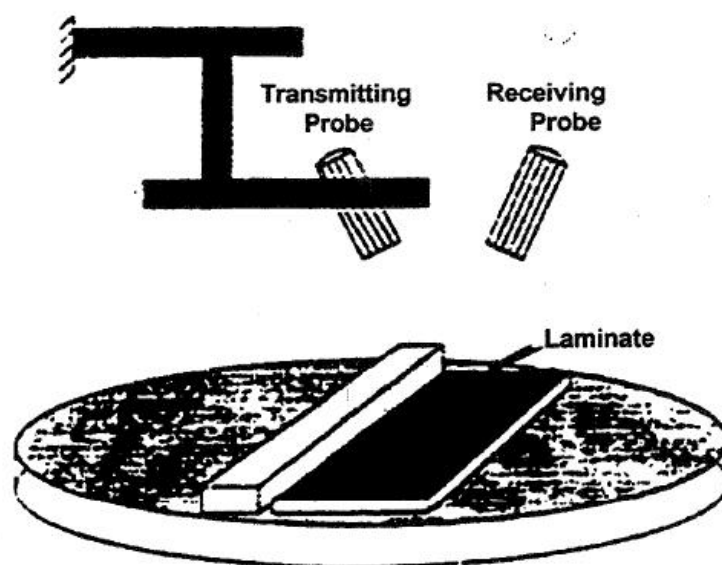


Figure 3.5.3. Setup for plate wave flow pattern method. (Sullivan et al. 1996)

The results showed that the waves propagate long distances along the fibers when compared with 90° (perpendicular) waves to fiber direction. Also, the beam spreading was more noticeable when the plate waves propagated across the fiber. Sullivan et al., demonstrated that the coupling between the inner and outer plies does not significantly affect the flow patterns even when more than one ply orientation exists in a laminated structure. The energy propagates along all fiber directions even in cases of specimens with fibers in many directions.

Since the fiber directions of the laminates had been successfully mapped, Sullivan et al. decided to investigate the response to different frequencies. A frequency analysis was conducted based on the principle that there are several modes that are simultaneously generated, and each mode has a unique displacement and stress profile across the thickness of the laminate. Hence, if individual modes are isolated, especially ones that have concentrated displacement/stress values across specific ply groups and knowing the mode shape of the displacement/stress, individual ply groups can be located. This portion of the study established that selective imaging of individual ply orientations using appropriate plate wave modes could be generated.

Sullivan et al. showed that the plate wave flow pattern technique was successful in mapping the fiber directions of a multi-ply laminate. They also developed a frequency-based analysis method to analyze the experimental plate wave flow pattern data. Using the frequency filtering method, they showed that the potential for a ply-by-ply fiber orientation analysis exists, if suitable parameters are selected. This technique can be used either as a local method or as a global scanning technique.

Michaeli, et al. (1999) used X-rays and image processing to determine fiber orientation of long-fiber-reinforced molding compounds in compression-molded parts. After a part was imaged, the X-ray was digitized and transferred to a personal computer for analysis. First, edge extraction was performed with the aid of differential operators. A gradient of gray-scale values exists between the fibers (bright areas in the X-ray) and the matrix (dark areas) that were used to detect the edge and thus the outline of the fibers. The edges of a fiber are characterized by high gray-scale gradients. For every pixel, the Sobel operator (calculates the difference between a given value and next-but-one neighbor) was used to calculate the

gray-scale gradients in the X and Y axes. The edges were detected by means of a defined threshold value. Only if the gray-scale gradient of a pixel exceeds the threshold value was an edge indicated. If the system determined that a pixel was lying on an edge, the direction of this edge and the orientation of the fibers was calculated. The number of detected orientations was counted for each angle between 1° and 180° and written as a histogram into a results file. The last stage in the X-ray image analysis consisted of calculating the fiber distribution function. Michaeli et al. concluded that the experimental and theoretical results showed that the X-ray and image processing system for measuring fiber orientation was sufficiently accurate and was suitable for verifying simulation results. Moreover, the system has proved to be an important quality assurance tool for several companies.

3.6 Fiber Waviness

Fiber waviness can be viewed as the through-thickness undulation of fibers in a thick section composite, and fiber waviness is a manufacturing defect that is introduced during manufacturing. Fiber waviness can occur during the filament winding process when wet hoop-wound filaments are under stress from the over wrapped layers or from buckling of prepreg. In addition, fiber waviness can occur during the cure cycle as a result of residual stress build up. Since fiber waviness can cause a significant reduction in strength and stiffness of the final product, nondestructive evaluation techniques are needed to detect and quantify this defect.

Chun and Jang (2000) investigated, both experimentally and theoretically, the use of convention ultrasonic to determine uniform fiber waviness in thick section composites. The authors studied a series of specially fabricated thick section graphite/epoxy composites with varying degrees of fiber waviness. There were three different degrees of fiber waviness that had fiber waviness ratios of 0.011, 0.034, and 0.059 where the fiber waviness ratio is the ratio of the amplitude of the fiber waviness to the wavelength of fiber waviness.

The authors used 10 MHz center frequency transducers in a through-transmission mode and measured time of flight and total energy received at different positions on the samples. The authors concluded from their numerical simulations and experimental data that the wavelength of the fiber waviness can be determined quantitatively by the relative distance between the peaks during scanning. In addition, they concluded that they could qualitatively determine the degree for fiber waviness by utilizing changes in the ultrasonic wave travel time.

Joyce, et al. (1997) extensively reviewed the literature for NDE techniques to determine fiber waviness in composites. The authors came to the conclusion that due to the complicated nature of acoustic wave propagation in wavy composites, the challenging problem of characterizing fiber waviness using ultrasonics remains largely unsolved. They also reviewed x-ray radiography and concluded that some success was demonstrated using embedded tracer fibers with a higher contrast to x-rays than the convention fibers and polymer matrix.

The authors then reviewed the literature on the use of optical microscopy to determine fiber waviness in carbon fiber composites and concluded that optical microscopy is the most powerful NDE tool currently available for determining fiber waviness in carbon fiber epoxy composites. Joyce et al. then experimentally developed and demonstrated an optical microscopy technique for determining the waviness in carbon/epoxy composite. They used an inverted metallograph at 80x magnification and dark field illumination to determine the amplitude and wavelength of the wrinkled regions.

They concluded that since most of the process induced fiber waviness in unidirectional thermoplastic laminates is clearly discretized into little fiber-wrinkled regions, the spatial distribution of fiber waviness can be estimated from surface inspection of the laminates by optical microscopy. However, it should be

stressed that this technique is operator dependent and also needs to be coupled with highly destructive and time-consuming sectioning of the composites to truly determine interior fiber waviness and any in-plane/out-of-plane character of the waviness. It therefore appears that this laboratory technique based on optically microscopy is severely limited for any use in manufacturing application.

To overcome the difficulties that are inherent in using 2D optical microscopy to determine fiber waviness in composite, Clark et al. (1995) developed a novel 3D optical method for determining fiber waviness in composites. They utilized a confocal laser-scanning microscope, which appears to be a very powerful technique for use in the laboratory to study and characterize fiber waviness on highly polished samples. However, it appears that the technique has severe limitations for use in manufacturing.

In summary, the authors concluded that the methodology to determine fiber waviness is limited to destructive analysis using optical microscopy. All of the NDE techniques based on ultrasonics, eddy currents or X-ray radiography should be viewed as works in progress, and they all currently have severe limitations in obtaining quantitative information.

Marshall and Hurmuzlu (1999) studied the use of radiographically opaque trace materials embedded in the lamina of composites used in manufacturing helicopters to image the fiber waviness. They concluded that this type of NDE approach showed the greatest promise (with the lowest impact to the manufacturing process) in detecting fiber waviness. The authors developed a PC-based visualization routine using computer assisted tomography, and coupled this with a computer program to view, analyze, and interact with the 3D representation of individual composite layers.

Kim, et al. (1998) developed analytic formulas for the ray path and travel times of an ultrasonic ray propagating in a wavy fiber-epoxy composite. They calculated them for rays initiating at various points with wave normal of differing directions. They experimentally determined that the arrival times observed by using various point like sources and point like detectors was in good agreement with those predicted by the theory of geometrical acoustics.

Wooh and Daniel (1994) studied the application of ultrasonics to characterize the fiber waviness in thick section composites. The authors studied a series of filament wound carbon/epoxy composites and destructively optically measured the amplitude (0.1") and the period (1.2") for machined surfaces of the samples. In addition, a reference sample was prepared with virtually no waviness. The authors reported that they were not successful in using conventional C-scanning or quantitative measurements to characterize the fiber waviness. They attributed this to refraction of the propagating ultrasonic beam.

To overcome this difficulty the authors used ray-tracing techniques. Figure 3.6.1 shows the ray-tracing map generated for a wavy layer composite. The authors were able to validate these ray-tracing maps by experiments, but they were only able to obtain qualitative and not quantitative verification of the ultrasonic results to the optical results.

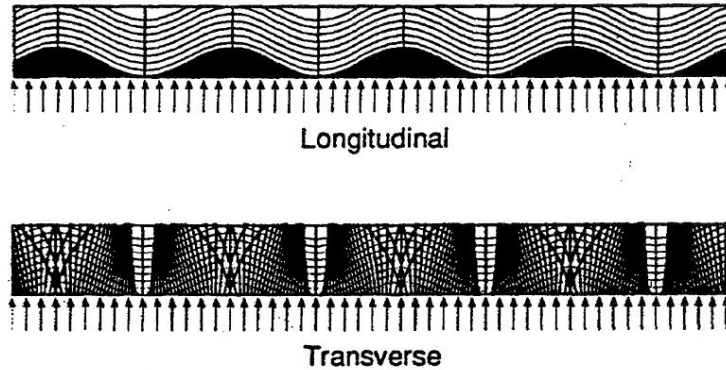


Figure 3.6.1. Trace maps of rays in 200-ply IM6G/3501-6 unidirectional lamina with wavy fibers. Woo and Daniels (1994)

4.0 NDE FOR IN-SERVICE DEGRADATION AND DAMAGE

The widespread use of composites is challenging NDE scientists and engineers to develop and validate quantitative methods for determining in-service degradation and damage in composites. Composite structures degrade over time in-service due to cyclic loading and the environment (e.g., water or water vapor). In addition, damage to composite structures in-service can occur through impact with foreign objects or through excessive heating. Also, composite structures, such as composite over wrapped pressure vessels (COPVs) that are exposed to long term, continuous high loads can fail due to stress rupture (sometimes referred to as creep rupture or static fatigue).

4.1 Delaminations

Delaminations are one of the most serious types of flaws that can occur in composites, and they lead to a substantial reduction in the compressive strength and mechanical stiffness. According to a Boeing study, by Miller, et al. (1994) about 60% of all damages found during the inspection of composite parts in airplanes are delaminations, which are typically caused by impact or critical loading. Delaminations can occur in-service from foreign body impact and cyclic loading, and/or they can also occur during manufacturing/processing from poor bonding (e.g., from contaminated prepreg) or from uncontrolled stresses during processing. Delamination is sometimes referred to as a crack-like discontinuity between plies and may propagate during use due to mechanical or thermal loading. In the worse case, the delamination may propagate and cause catastrophic fracture of the component. Therefore, the nondestructive evaluation of delaminations is very important in both the manufacture and in-service sustainment of these materials.

A number of NDE techniques have been used to detect and evaluate delaminations. Techniques that are well established include: visual inspection, tap testing, resonance methods, various ultrasonic methods, thermography, eddy current testing, shearography, and x-ray radiography. However, inspection of composites is a difficult task due to their multi-layered structure, anisotropy and heterogeneity, and therefore, research and development to improve NDE techniques to detect and quantify delaminations is continuing on at a number of laboratories.

Petculescu and Achenback (2007) and Petculescu, et al. (2007) reviewed the results of their research on using Lamb-waves to detect and quantify delaminations in woven quasi-isotropic carbon/epoxy composites. The authors used the lowest antisymmetric lamb mode excited in a zone with minimal dispersion at a wavelength of 4.5 mm in a test to detect and size simulated midplane delaminations in

woven quasi-isotropic carbon/epoxy composites. The midplane delaminations were simulated by circular inserts of various types and sizes introduced into the panel's midplane during fabrication.

The lowest lamb mode propagation characteristics in the composite, with and without the midplane delaminations were analyzed. The change in the mode's group velocity was used as a damage indicator and the accumulated time delay of the traveling ultrasonic pulse was used for size estimation of the delaminations. The authors reported that the results are repeatable and constant, and suggested that time delay is a potentially reliable damage parameter for quantitative monitoring of delamination in composites.

There are currently a number of research activities that are focused on developing and applying digital shearography for nondestructive evaluation of composites in production and field environments. Yang (2006), in a view article, described the technique and highlighted the technique's potential and limitations. Figure 4.1.1 shows the fundamentals of digital shearography. A typical setup of digital shearography in which a modified Michelson interferometer is used as a shearing device is shown in Figure 4.1.1 (a), and the author provides the equations that go along with this Figure.

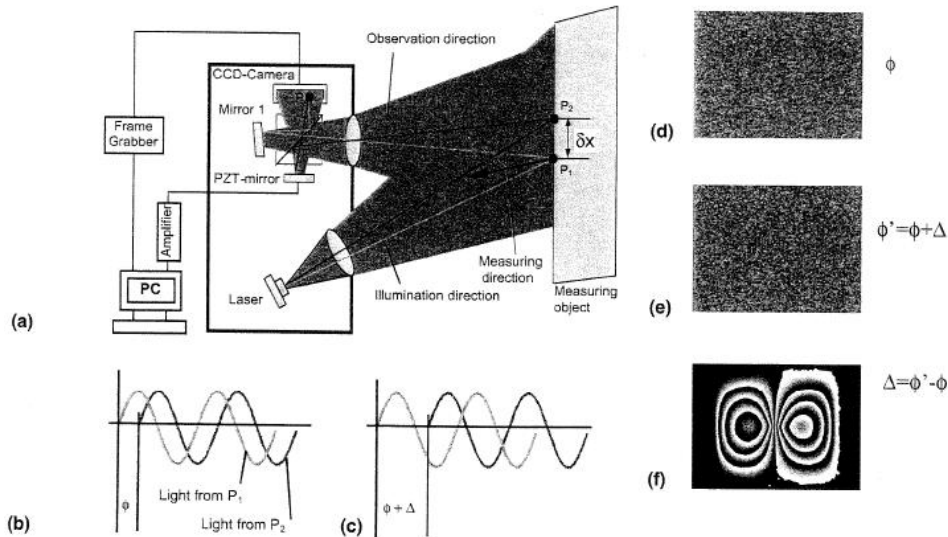


Figure 4.1.1. Fundamentals of digital shearography: (a) schematic of a typical digital shearography setup using a modified Michelson interferometer as a shearing device; (b) interference phase ϕ before loading; (c) interference phase $\phi' (= \phi + \Delta)$ after loading; (d) the calculated phase distribution ϕ for a square plate clamped all around and loaded centrally; (e) the calculated phase distribution ϕ' ; (f) the relative phase change obtained by subtracting ϕ from ϕ' . (Yang 2006)

Yang (2006) also provided a description of practical applications for digital shearography including disbonds and delaminations in composites. The author also reviewed the different loading methods that can be utilized with digital shearography, which included: vacuum loading, thermal loading, internal pressure, and dynamic loading (harmonic and nonharmonic via a piezoelectric transducer with an amplifier or a shaker). Digital shearography is a full field technique and is therefore, very rapid. It also has a high reliability for finding smaller, deeper (less than 1 or 2 mm) flaws than can be found with the older, electronic shearography. The author stated that the application of digital shearography to composites is increasing and a wide range of applications will emerge in the future.

Weigl, et al. (2000) compared the capability of digital shearography and electronic speckle pattern interferometry (ESPI). Both ESPI and digital shearography are laser light based, full, field, non-

contacting, optical interference techniques. When applied, the results are a set of optical fringe patterns, which are representative of an objects surface displacement in response to a mechanically applied stress. The presence of a defect locally influences the object's surface deformation when stressed which, in turn, can be detected in the fringe patterns produced.

The shearography process, which measures the object's surface deformation, is shown in Figure 4.1.2. Laser light, which reflects off the illuminated object surface, is viewed through a set of shearing optics. The function of the shearing optics is to laterally shear the image of the object into two overlapping images. This causes the two images to interfere and produces a unique speckle pattern, which is captured and digitized by a computer.

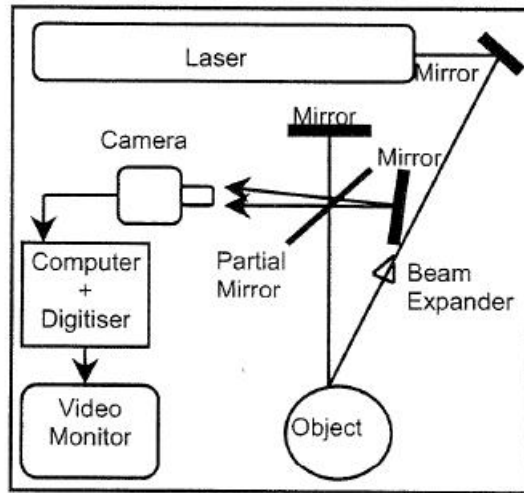


Figure 4.1.2. Typical shearography set-up. (Weikl, et al. 2000)

On the other hand, the authors point out that ESPI uses a separate object and reference beam to record surface displacement of an objects surface in response to the applied force. The set-up for ESPI is shown in Figure 4.1.3. By comparing the speckle interference pattern of an object both before and after object stressing, areas of correlation and decorrelation produce the familiar zebra-striped pattern.

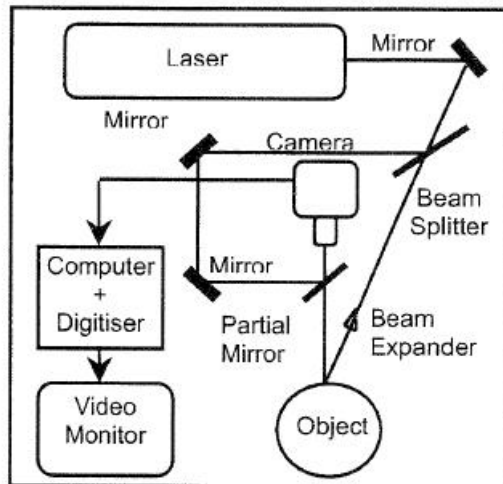


Figure 4.1.3. Typical ESPI set-up. (Weikl, et al. 2000)

Weigl, et al. used layered composite samples with a length of 20 cm and a width of 2 cm that consisted of 8 or 10 layers of unidirectional carbon fiber reinforced plastic (Hexcel Composites, Fibredux 913C), which is also used in Airbus planes. Starter delaminations were introduced in the samples by using Teflon foil as a starter defect and then applying a large tensile overload load to introduce damage in the form of delaminations. In all cases the samples were loaded under pure plane tension to obtain the stressed condition for the tests. Figure 4.1.4 shows the ESPI image of a sample with the initial Teflon delamination region marked by the two crosses and the larger delamination region that was produced by the applied damage overload. Figure 4.1.5 shows the same sample via a shearography measurement, and Figure 4.1.6 shows the actual out-of-plane displacement information obtained using a reconstruction algorithm to remove the image shearing and get a real displacement image. The authors stated that the results show that both shearography and ESPI are well suited for the detection of delaminations in layered composites.

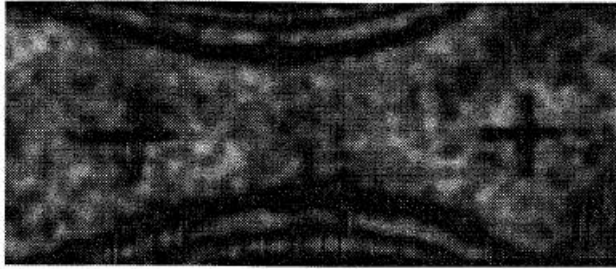


Figure 4.1.4. ESPI of a damaged $[\pm 45, 0, 90T]_s$ sample. (Weigl, et al. 2000)

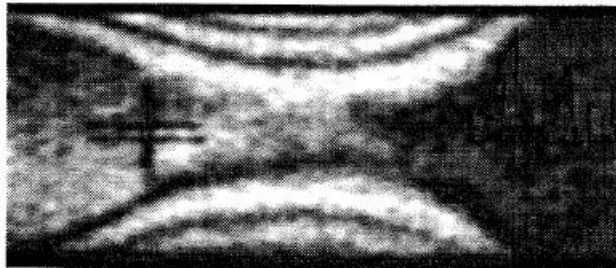


Figure 4.1.5. Shearogramme of the same sample as in Figure 4.1.4. (Weigl, et al. 2000)

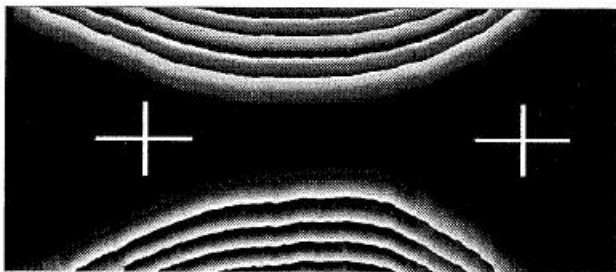


Figure 4.1.6. Reconstructed displacement field of Figure 4.1.5. (Weigl, et al. 2000)

In a later effort, Weigl and Schnack (after 2000) were able to show that a quantitative determination (i.e., size, shape and location) of delaminations can be obtained by solving the inverse problem. The authors developed a new reconstruction algorithm for use in obtaining the quantitative informant on delaminations.

Smith et al. (2000) studied the use of ultrasonic pulse echo amplitude to size delaminations in fiber-reinforced composites. The authors studied the simple amplitude method within the near field of a transducer for sizing delaminations where small defects are sized by measuring the amplitude of the signal reflected from the defect. A theoretical treatment of the measurement was verified experimentally with delaminations of known sizes. The authors used a standard reference panel, shown in Figure 4.1.7, in their experimental studies. In this Figure, the top three rows of defects are fabricated using two layers

of 50 μm -thick PTFE sealed around the edges with heat-resistant tape, whilst the other defects are single layers of 50 μm -thick release film. Nominal widths and diameters of the inserts are 25, 12 and 6 mm.

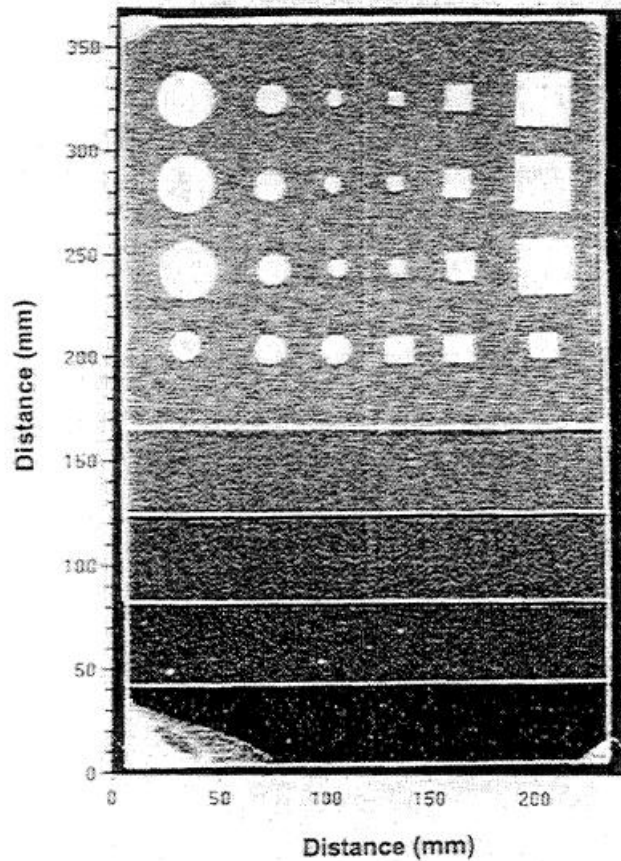


Figure 4.1.7. Double through-transmission scan of the NPL-designed standard reference panel with 24 reference defects and stepped thicknesses of 5, 4, 3, 2 and 1 mm. (Smith et al. 1997)

Despite verifying the theoretical treatment experimentally, the authors believe that the amplitude method is not to be recommended for delamination sizing in fiber-reinforced composites because of the large uncertainty levels in the results. The authors conclude from their study that errors of 20% in defect area were caused by an error of only 1.85 dB in the reflection coefficient of a delamination. In addition, the inhomogeneous nature of composites and the variable reflection coefficients of defects have resulted in random errors of plus or minus 40% in the estimated defect area.

Hesiehurst et al. (1998) applied a new portable holographic interferometry testing system to determine the location and direction of growth of delaminations in composite panels. Figure 4.1.8 shows the holographic interferometry system layout used by the authors.

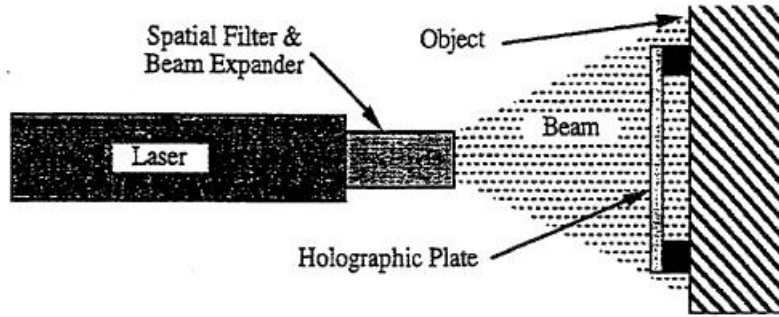


Figure 4.1.8. Holographic interferometry system layout. (Hesiehurst et al. 1998)

Holographic interferometry can be used to determine the contour shapes of the out-of-plane displacements of a surface. Hesiehurst et al. used reflective holographic interferometry, which is an optical method that produces an interferometric fringe pattern superimposed on the region of interest. The fringe lines represent points or lines of equal out-of plane displacements. The horizontal distance between each fringe represents a vertical distance equal to half the wavelength of the emitted laser light (on the order of 0.6328 micrometers when using a helium-neon laser). The procedure for producing a holographic interferogram is relatively straightforward: 1) a holographic plate is attached to the region of interest, 2) after applying an initial load, the holographic plate is exposed to the laser light, 3) the load is marginally increased and the plate is exposed for a second time, 4) the holographic plate is then developed, and 5) the developed holographic plate is then viewed using reflected white light.

Hesiehurst et al. used this methodology to study delamination of composites under compressive load and concluded that this holographic technology can be used to determine the location of the site with maximum out-of-plane gradient of the delamination buckle. When viewing a hologram, this site is the likely spot for delamination propagation. They also concluded that the characteristic shape of the delamination buckle would indicate the direction of delamination growth. Although the authors used this technique in a laboratory study to enhance the understanding of the delamination process, they speculate that it is also applicable to determining the severity of delamination in composite structures.

Several authors have used electrical measurements to characterize delaminations in carbon fiber composites. Todoroki et al. (1995) used the electric potential method to detect delaminations. The authors used the electric bridge circuit approach to determine changes in electrical resistance as a function of delamination or crack length. The authors conclude that this type of NDE measurement is excellent for detecting delaminations in aircraft structures. This technique only requires low currents so the composite structure is not heated. However, electrodes must be attached to the composite for inspection.

In a similar study, Wang and Chung (1997) used electrical resistance measurements with four point probe instrumentation to sense delaminations in carbon fiber composite. The authors concluded that the sensing of delaminations in a cross ply (0/90) continuous carbon fiber polymer composite during fatigue was demonstrated in real time by electrical resistance measurements in the through thickness direction. Figure 4.1.9 shows the variation in resistance, $\Delta R/R_0$ as a function of % fatigue life.

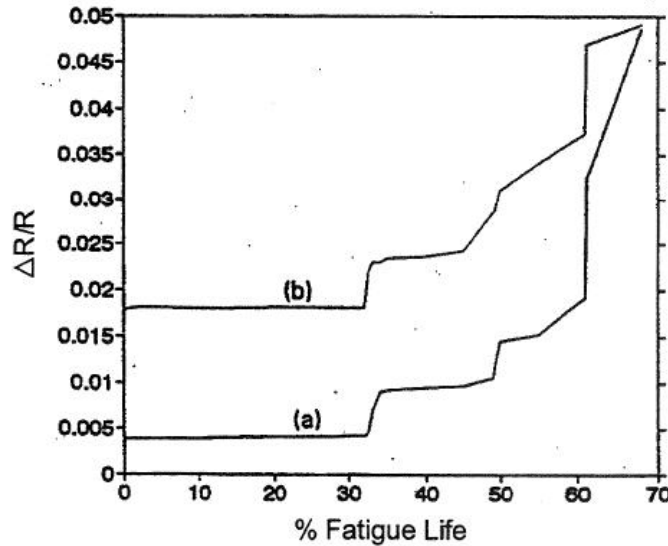


Figure 4.1.9. Variation of $\Delta R/R_0$ in the through-thickness direction with the percentage of fatigue life during tension-tension fatigue for a crossply composite. (a) Minimum $\Delta R/R_0$ at the end of a cycle. (b) Peak $\Delta R/R_0$ in the middle of a cycle. (Wang and Chung 1997)

Gros and Takahashi (2000) have investigated the use of Foucault currents, commonly referred to as eddy currents, to detect and quantify delaminations in carbon fiber polymer composites. The authors made note of the fact that at the 1993 European meeting of the Annual Congress of Civil Aviation plans were developed for an R&D program on eddy current NDE for assessing the integrity of carbon fiber polymer composites. The authors used a commercial eddy current instrument with a high frequency (2MHz) and a small probe diameter (2 mm) with manual scanning in their experiments. They characterized delaminations in a 24-mm by 14-cm by 1.14-mm thick specimen. The frequency could be selected to control the depth of penetration of the eddy currents. The specimens were quasi-isotropic laminates with a layer arrangement of (0/ -45/+45 /90 degree) and had real delaminations introduced by tensile load. The delaminations apparently were characterized by optical microscopy at the edges of the sample and these results were compared to the eddy current results. The authors concluded that eddy current testing is a potential method for the nondestructive detection and characterization of delaminated area at interfaces between plies in carbon fiber/epoxy laminates.

A number of researchers have investigated the feasibility of embedding optical fibers into composites for the purpose of health monitoring of composite structures for delaminations. Sirkis et al. (1994) investigated the effects of embedding optical fibers in graphite/epoxy laminated composite panels. They embedded optical fibers ranging in size from 80 to 600 micrometers at the laminate mid-plane. They then subjected the panels to low velocity impact damage to induce delaminations. With the exception of the 600 micrometer optical fibers, they found that the optical fiber sensors embedded in the mid-plane of the laminates did not influence the size or distribution of the delamination damage. The authors used x-ray radiography, ultrasonic C-scans, and volume visualization to determine if the embedded sensors influenced the macroscale delamination damage in composites.

Elvin and Leung (1997) carried out a theoretical study of the feasibility of using embedded fiber optic sensors to monitor for delaminations in composites. The authors used a physical modeling of the measurement method approach to reach their conclusions. As a result of their modeling efforts, they conclude that the very small incremental changes in the length of embedded optical fibers can be used to determine the size and location of delaminations in fiber composites.

Park et al. (2000) studied the use of embedded extrinsic Fabry-Perot interferometer optical fiber sensors to detect delamination and buckling in composites. Figure 4.1.10 is a schematic of the fiber optic sensor constructed by the authors. These sensors had a diameter of about 250 micrometers and were constructed using single mode and multi mode fiber that were connected together by using a quartz capillary and epoxy. The space between the ends of the fibers was controlled to give Fresnel reflection (about 10 to 50 micrometers). The sensors were embedded in graphite/epoxy laminates that were then subjected to compression test. The authors concluded that the compression tests of the composite beams with the embedded fiber optic interferometer were successful. They also concluded that these sensors are a powerful tool that can be used to identify the onset of buckling and delamination in composites.

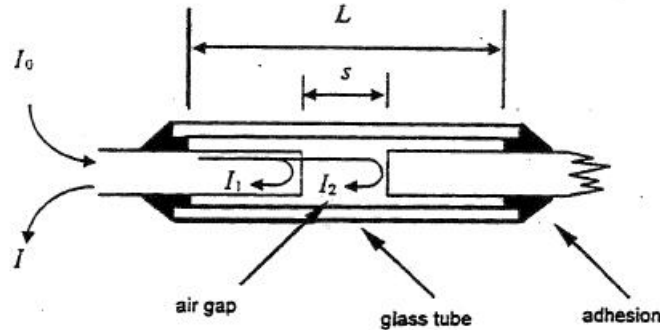


Figure 4.1.10. Schematic diagram of fiber optic sensor. (Park et al.2000)

Mian, et al. (2004) studied the application in composites of utilizing a short ultrasonic pulse to heat fatigue damage including delaminations and to the image the heat liberated via IR-thermography. The technique uses a short (200 msec) sound wave pulse (20 kHz) to heat the flaws by internal friction. The authors used sample panels made of epoxy reinforced with woven carbon fiber and manufactured by the resin transfer molding process. The panels were nominally 3.0 mm thick and had a fiber volume fraction of 0.55. Delaminations were introduced by cyclic fatigue testing. Figure 4.1.11 shows a schematic of the sonic-infrared imaging technique.

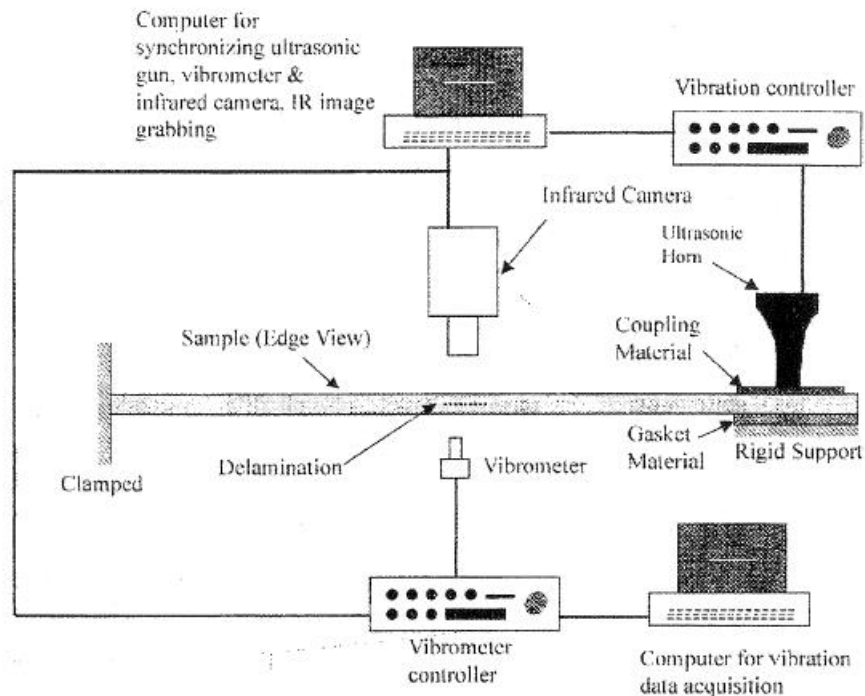


Figure 4.1.11. Schematic diagram of sonic-infrared imaging technique.

The authors were able to obtain good correlation detecting fatigue damage in composites between using the sonic infrared imaging technique and the more traditional thermal wave imaging technique.

Lipetzky and Bandos (2003) reported on the inspection of composite structures for naval applications. They used a leaky Lamb wave approach to detect kissing bonds and delaminations in composite panels. The authors reported that they were able to relatively successfully detect and size delaminations in their leaky Lamb wave scans.

Sugimoto, et al. (2005) studied the application of x-ray computed tomography to detect delaminations and other small defects in composites such as voids and matrix cracking. The authors used a Micro CT system with a scan area of 200 mm x 300 mm with a minimum pixel size of 5 x 5 microns for a 3 mm scan area. The voltage could be varied from 30 to 225 kV and the current could be varied from 10 to 500 micro A. Positions of the test sample and the X-ray image intensifier are also variable and this makes continuous zoom possible. They were able to detect and size cracks/delaminations in carbon/carbon composites and voids in CFRP composites.

Songling, et al. (2003) used infrared thermography to study delaminations in honeycomb aluminum composites. Their samples had a cover aluminum skin that was 0.5 mm thick, and the honeycomb was hexagonal with sides of 5.0 mm, and the honeycomb was 0.1 mm thick. The authors made simulated delaminations in the honeycomb by placing polyethylene slices that were 16 mm diameter, and 20 micros thick between the cover skin and the honeycomb.

4.2 Impact Damage

Nondestructive detection and characterization of impact damage is an important issue in utilization of fiber reinforced composites. For example, it is not uncommon for composite structures to exhibit invisible front surface damage from foreign object impact but have extensive back surface damage. The ability to characterize nondestructively the impact damage and predict the residual strength of the

damaged structure is of major importance for an effective damage tolerant design and provides also tools for in-service supportability. Gottesman and Firshovich (1998) have reported development of an analytical damage model for thick laminates loaded in compression. The mechanical damage model was based on damage assessment evaluations provided by ultrasonics and a destructive x-ray microfocus technique combined with an opaque penetrant for damage enhancement. Using the mechanical damage model, a failure model was constructed that led to failure prediction. The analytical models were successfully verified experimentally for various materials impacted at different energies. Gottesman and Girshovich suggested that the combination of nondestructive damage characterization and analytical modeling enables the evaluation of the degradation of the mechanical behavior of impacted composites laminates.

Earlier work by Zalameda et al. (1994) demonstrated that a multi-disciplinary approach for impact damage detection in composite structures can provide a reasonably efficient inspection. In this work, a thermal inspection technique was used to rapidly identify the impact damage and ultrasonic volumetric imaging quantified the impact-generated delaminations through the volume of the structure. In more recent work by Ball and Almond (1998), the possibility was explored of using transient thermography along with image analysis approaches to detect impact damage in thicker composites. Carbon fiber reinforced plastic (CFRP) laminates ranging in thickness from 3.44 mm to 13.76 mm were investigated. Laminates damaged by low velocity impact were examined with transient thermography and a commercial image processing package and the results compared with ultrasonic c-scans and sectioning. The thermography images demonstrated the ability of the technique to detect the presence of impact damage in all of the specimens examined. Damage area estimates from front face thermographic images correlated with measurements of sub-surface damage obtained from sectioned samples but did not correlate with the c-scan results. Damage areas produced by back face thermographic images correlated well with those obtained from sectioned specimens as well as with C-scans for thinner specimens but not for the thicker (13.76 mm) specimens. Based on plots of thermographic damage area vs. C-scan damage area, Ball and Almond suggested that a minimum threshold damage size exists which is not detectable by transient thermography using the equipment and methods applied in their work.

In further development of thermographic inspection approaches for composites, a report by Bai and Wong (2001) discusses the use of lock-in thermography. Lock-in thermography utilizes an infrared camera to detect the surface temperature of a thermal wave propagating into the material and then produces a thermal image, which displays the local variation of the thermal wave in phase or amplitude. Defects are detected by differences in phase or amplitude between defective areas and non-defective areas. As in most nondestructive inspections, parameters should be optimized to minimize the difference between defective areas and non-defective areas. The phase difference depends on the thermal properties of the material, the subsurface structure of the sample, the modulation frequency and the surface heat transfer coefficient. Also, in real applications, such as inspection of aircraft structures, the effect of surface convection caused by airflow in natural ambient environments can be significant for some thin structures in which the dominant mode of heat transfer is convection. In order to better understand the behavior of thermal waves under these conditions, Bai and Wong developed a photothermal model for lock-in thermographic evaluation under convective conditions of CFRP plates of finite thickness in which defects were implanted. Experiments were performed to verify the photothermal model and determine the detectivity of lock-in thermographic inspection of the plates. The CFRP specimens were 300 mm x 300 mm x 4.2 mm thick. Artificial defects comprising Teflon films 0.2 mm thick were implanted in the specimens. Defects with diameters ranging from 1 mm to 11 mm were inserted at depths ranging from 0.28 mm to 2.8 mm. A comparison of experimental results obtained from the 11-mm diameter defect at a depth of 0.56 mm and the theoretical results obtained with the photothermal model are shown in Figure 4.2.1.

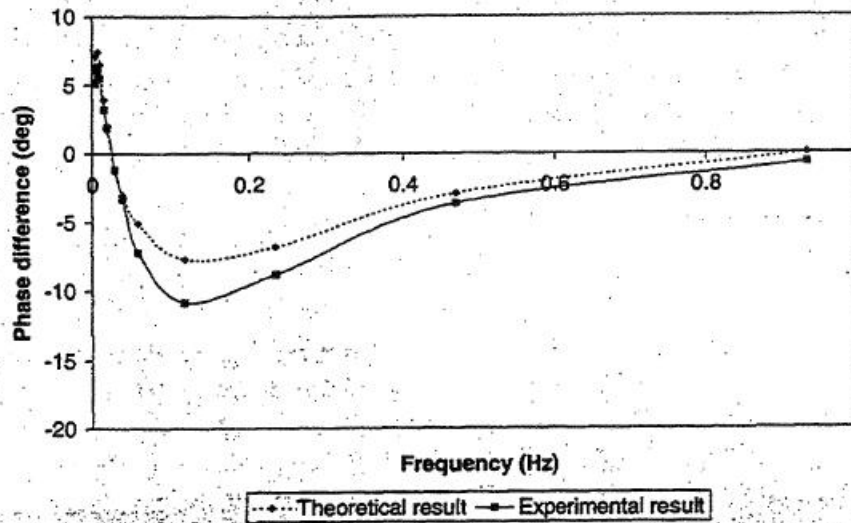


Figure 4.2.1. Experimental and theoretical phase differences between defective areas and non-defective areas produced by a 11-mm diameter defect at a depth of 0.56 mm. (Bai and Wong 2001)

In this Figure, the phase differences between the central point of a defect image and the average phase value of its surrounding were calculated as the experimental result. As can be seen, although the theoretical and experimental results have similar trends, the phase differences obtained experimentally are larger than those obtained theoretically; this was the case for all defect depths. Bai and Wong attributed this discrepancy to ignoring thermal contact resistances between interfaces owing to the difficulty in determining these numbers. This would be expected to lead to more conservative predictions. The authors found that there are frequencies for a specific defect at a certain depth where the phase difference produced by the defect is very small, or zero, and other frequencies where maximum positive and negative phase differences are produced. Also the optimum frequencies change with depth and the deeper the defect the lower the optimum inspection frequency. Since, the optimal frequencies obtained theoretically are very close to those obtained experimentally, the photothermal model can be used to predict optimum inspection frequencies and is useful for selection of inspection parameters.

In recent years, additional work has been done to improve the quantitative capability of thermographic inspection. The introduction of the infrared camera in the late 1960's simplified the acquisition and visualization of transient surface temperature data, enabling the practice of active thermography for qualitative identification of subsurface flaws. However, the principles of heat conduction can be applied to the data sequence to measure various thermophysical properties of the sample, including flaw depth and size, sample thickness and thermal diffusivity. Modern quantitative methods typically employ flash thermography, and involve measurement of the times at which signal events associated with subsurface anomalies occur.

Although many approaches to quantitative thermographic NDT have been reported and discussed in the literature, relatively few have been implemented to any significant extent. The following describe approaches that have achieved some degree of consensus in the composites community.

Although developed in 1960, variants of the "Parker method," Parker et al. (1961), are still widely used to measure through the plane thermal diffusivity in planar, or near planar solids. It is a 2-sided process that involves application of a heat pulse to one face of the test piece, and measurement of the resulting temperature rise on the opposite side. The time at which the temperature reaches half of its maximum

value is measured and thermal diffusivity is calculated. While the original method was a single point measurement, modern versions employ IR cameras and extended sources to provide wide area, non-contact diffusivity measurement.

Using a Wiener-Hopf solution for a lateral crack, Almond and Lau (1994) demonstrate that the apparent diameter of a subsurface flaw will decrease as time progresses. However, accurate sizing may be achieved by correcting the measured full width at half maximum (FWHM) of the image contrast.

Early approaches to depth or thickness measurement required identification of a defect-free reference point on the test piece, or inclusion of a reference sample in the field of view. Quantification was achieved by measuring the maximum slope of the contrast curve. Ringermacher and Howard (2001) create a synthetic reference based on known 1-dimensional diffusion behavior for a plate sample, which is a straight line with slope -0.5. The contrast of each pixel with respect to the synthetic reference is calculated and differentiated in order to find the inflection point of the contrast curve slope.

Work reported by Shepard et al. (2006) describes the Thermographic Signal Reconstruction (TSR) method, which is widely used to improve sensitivity compared to raw image output, and to measure depth / thickness or thermal diffusivity, based on the behavior of the logarithmic time derivative of each pixel. Measurement of thickness and diffusivity using the second derivative is demonstrated, and diffusivity results compare favorably to those achieved using the Parker method, described above. The shape and polarity of the derivative is shown to indicate whether a subsurface feature is a discrete flaw where 2-dimensional heat flow occurs as heat flows around the feature (bipolar signal), or an extended interface, where the interaction is purely 1-dimensional (positive unipolar derivative signal).

Another approach to non-contact, whole-field, real-time characterization of impact damage in composite materials is electronic speckle pattern interferometry (ESPI) as described by Richardson et al. (1998). ESPI is one of a family of coherent light interferometry techniques that also include holographic interferometry, speckle interferometry and speckle shearography. Each is capable of measuring either surface displacement or displacement derivatives with practical benefits of being able to make whole-field, non-contact measurements. ESPI has potential for detection of defects in composite materials due to its advantages of real-time measurement, electronic output as well as the direct indication of defect features. Richardson et al. investigated the applicability of using ESPI intensity fringes and phase maps to evaluate internal damage in glass fiber reinforced polyester composite materials. An illustration of their experimental setup is shown in Figure 4.2.2.

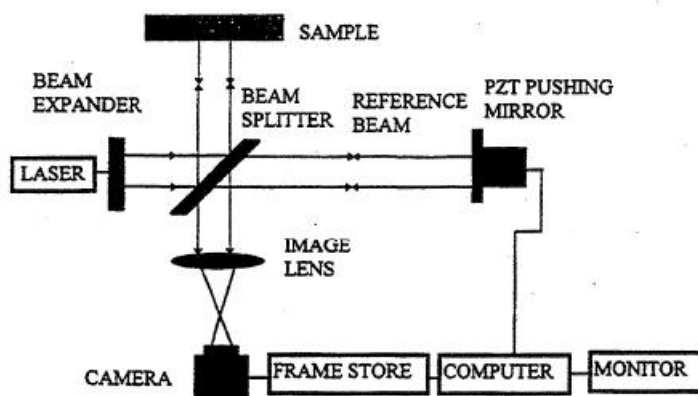


Figure 4.2.2. Optical configuration of phase stepping ESPI. (Richardson et al. 1998)

Phase maps were produced in parallel with intensity fringes to show damage features as well as to indicate the difference between intensity fringes and phase maps in terms of visibility and readability. Both the intensity fringes and the phase maps show the existence of internal damage. The dynamic variation of intensity fringe patterns associated with defects can be readily monitored in real time. Unfortunately, they are not always of good visibility because the spatial frequency distribution of a speckle pattern containing the data signal is embedded in noise. Another problem is the interference of rigid-body-movement-induced background fringes not associated with the damage. On the other hand, fine details of damage can be easily visualized using phase maps with very high visibility and readability as shown in Figure 4.2.3. Damage areas in the specimens were verified using ultrasonic C-scan and sectioning. Test results from an ultrasonic C-scan are shown in Figure 4.2.4 and damage profiles determined using sectioning are shown in Figure 4.2.5. These test results bear close geometrical resemblance to both the intensity fringes and phase maps from ESPI (see Figure 4.2.3); however, there are notable differences in terms of calculate damage areas as shown numerically in Table 4.2.1.

Although phase maps can be directly linked with damage and are straightforward to interpret, real-time observation cannot be achieved due to intensive post-processing computation. Richardson, et al. point out that in the broader scientific sense, in the case of phase mapping there is the potential to extract information from the computer that which could quantify the level of damage and which could be used to alert, say a quality control operator, to the need to make further decisions thus providing an automated nondestructive inspection approach.

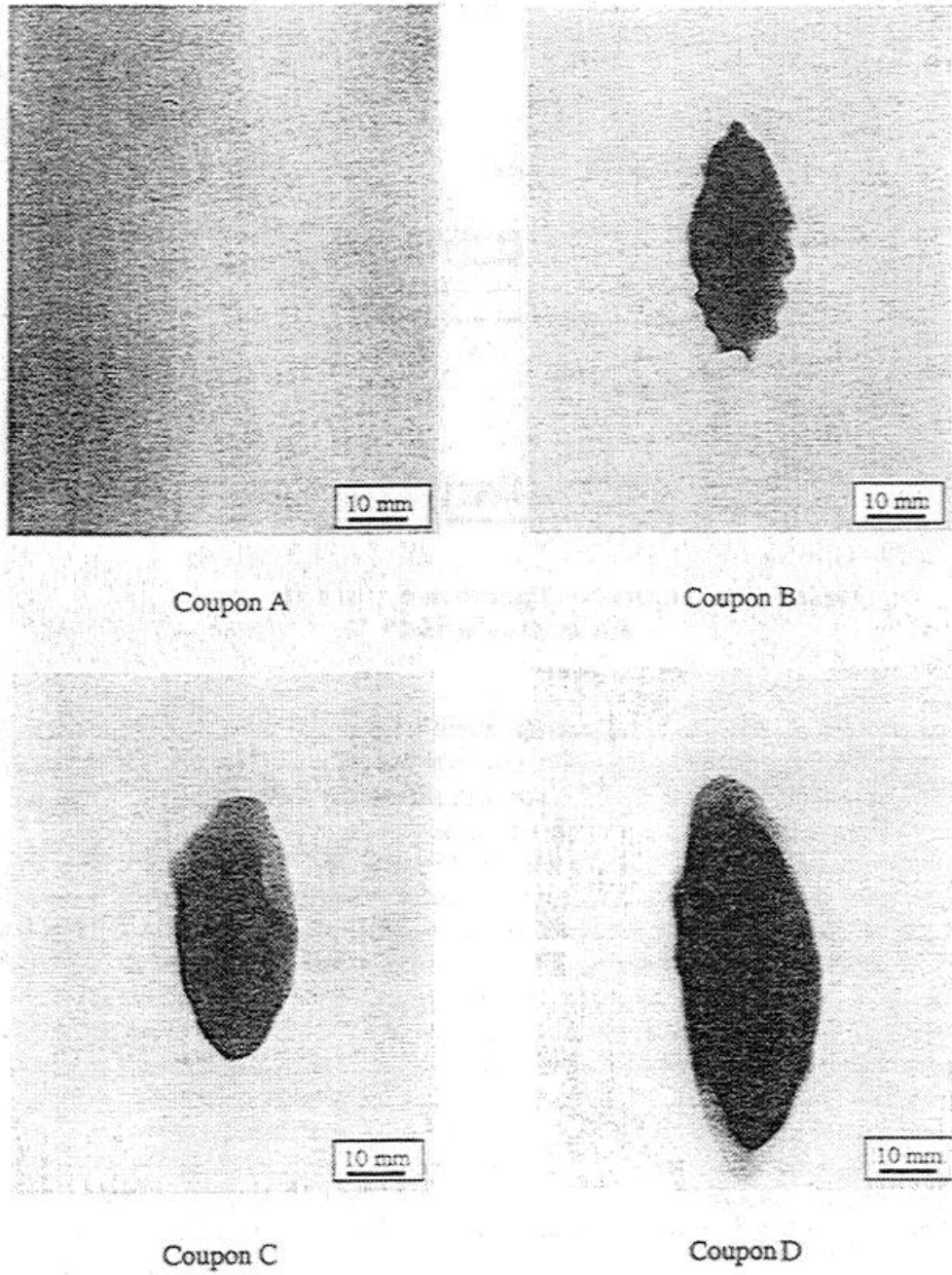


Figure 4.2.3. Phase maps of four impacted coupons. (Richardson et al. 1998)

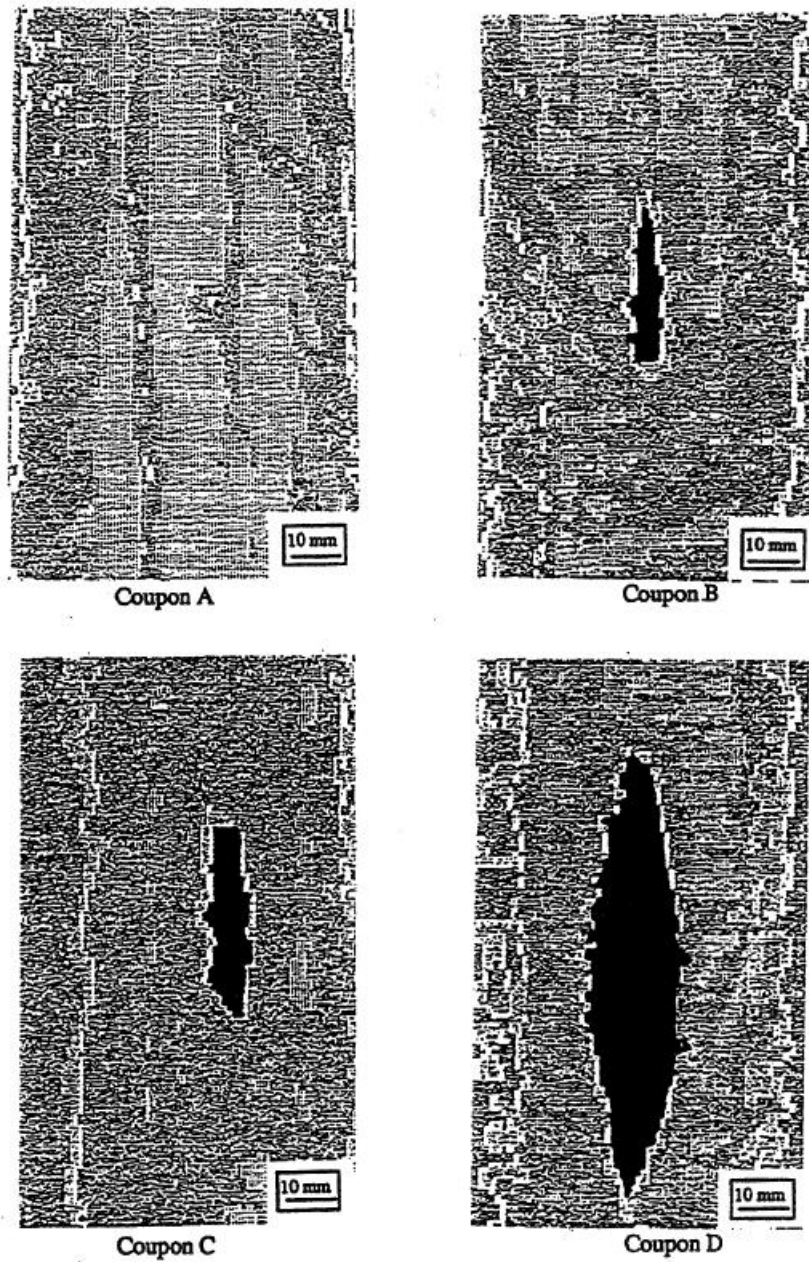


Figure 4.2.4. Damage profiles detected by ultrasonic C-scan. (Richardson et al. 1998)

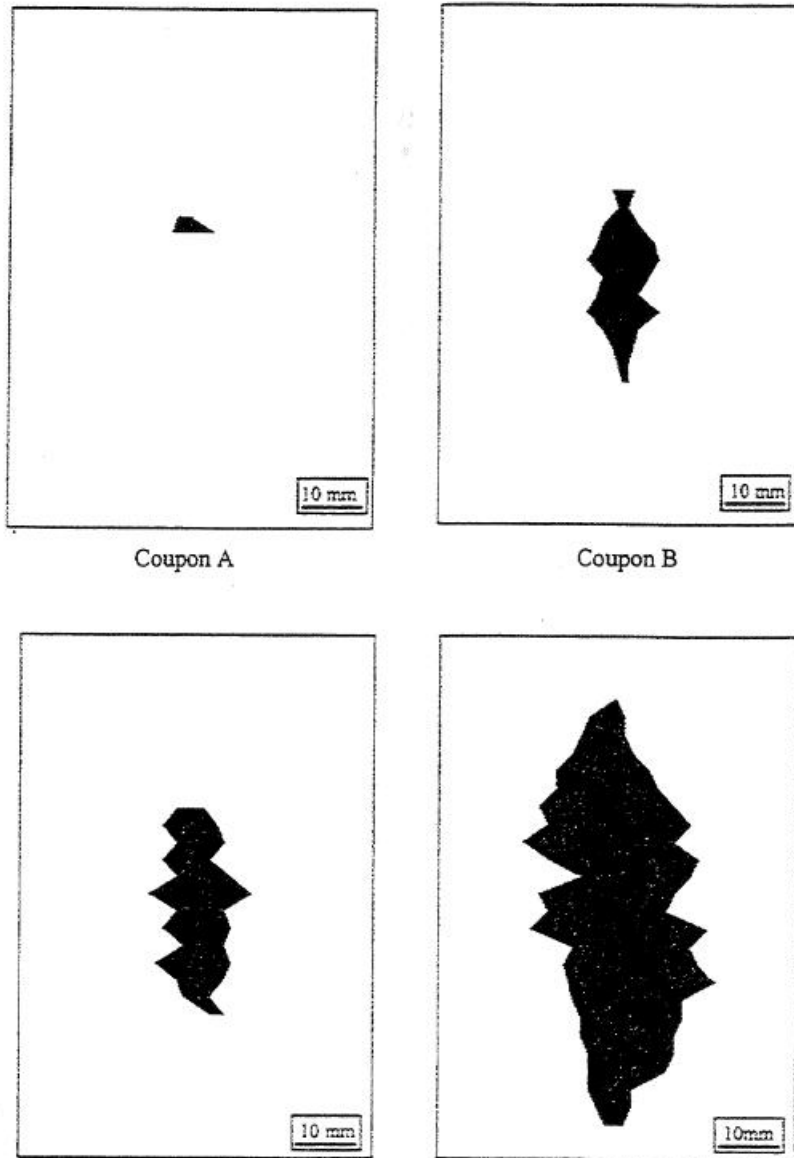


Figure 4.2.5. Damage profile of impacted coupons by sectioning technique. (Richardson et al. 1998)

Table 4.2.1. Comparison of damage areas determined by intensity fringes, phase maps, ultrasonic C-Scan and sectioning techniques. (Richardson et al. 1998)

| Test Technique | Damage area (mm ²) | | | |
|------------------|--------------------------------|----------|----------|----------|
| | Coupon A | Coupon B | Coupon C | Coupon D |
| Intensity fringe | 0 | 188 | 256 | 9325 |
| Phase map | 0 | 194 | 270 | 975 |
| C-scan | 0 | 156 | 227 | 1168 |
| Sectioning | 0 | 223 | 330 | 1245 |

Bar-Cohen and Lih (2000) also reported the use of leaky Lamb waves to detect and quantify delaminations and other defects in composites. The authors reviewed their efforts over the past 17 years to develop and utilize leaky Lamb waves (LLW), however they pointed out that these techniques using

oblique insonification of composites are still not used routinely in industrial application. The LLW phenomenon is associated with a resonant excitation of plate waves that leak waves into the coupling fluid and interfere with the specular reflection. The leaky waves modify the reflection spectrum introducing a series of minima produced by a destructive interference at specific frequencies between the leaky wave and the specular reflection. The LLW procedure involves measuring the reflections and extracting the dispersive characteristics at various angles of incidence and at several orientations (polar angles) with the laminate fibers. The data is presented in the form of dispersion curves showing the LLW modes' phase velocity (calculated from Snell's law and the angle of incidence) as a function of frequency.

Bar-Cohen Cohen and Lih pointed out that the experimental acquisition of dispersion curves in composites requires accurate control of angle of incidence/reception and the polar angle with the fibers. In this paper, they reported on their recent successful efforts to enhance the speed of LLW data acquisition. In addition, they reported on their successful efforts to develop an algorithm to optimize the height of the two ultrasonic transducers used so that the beams cross precisely on the surface of the specimen. The authors showed their data, successful obtained at high frequencies, for the determination of porosity in a Gr/Ep [0] 24 laminate. In addition, they presented data on a similar Gr/Ep [0] 24 laminate and were able to show that they could follow a reduction in Young's modulus when the laminate was heat-treated. The authors concluded by listing the three issues that have hampered the transition of LLW to industrial use for composites: 1) need to determine density of the composite from a single sided NDE measurement (this is still an unresolved issue; 2) the data acquisition process needs to be more user friendly and faster (the authors claim significant progress on this issue); 3) The inversion technique for determining the elastic stiffness should be applicable to multi-layer composites in terms of global properties (the authors claim some progress on this issue).

Amaro, et al. (2004) did a comparative study of different NDE techniques applied to the characterization and quantification of impact damage in carbon-epoxy composites. The authors choose electronic speckle pattern interferometry (ESPI), shearography and ultrasonic C scan for their comparison testing since they believed that these techniques were the most likely to be able to detect and quantify low energy, impact damage in composites. They used a drop weight-testing machine to introduce low energy impact damage in the carbon-epoxy 16 ply laminate plate Samples with two different types of stacking sequence. A 20 mm diameter ball was used with impact energies of 1.5 J, 2 J, 2.5 J and 3 J that corresponded to loads of 2160 N, 2430 N, 2700 N and 2970 N.

Table 4.2.2 shows the average size of impact defects from all of the inspected panels by the three NDE techniques. It should be noted that there are pronounced differences between the ultrasonic technique and the interferometric techniques. However, all of the techniques showed increasing damage with increasing impact energy.

Table 4.2.2. Defect size from the NDT techniques. (Amaro, et al. 2004)

| Energy [J] | Delaminated area [mm ²] [0,90,090] _{2s} | | | Delaminated area [mm ²] [0,90] _s | | |
|------------|-----------------------------------------------------------------|-------|--------|------------------------------------------------------------|-------|--------|
| | ESPI | SHEAR | C-SCAN | ESPI | SHEAR | C-SCAN |
| 1.5 | 144 | 115.2 | 184 | 60.5 | 63.1 | 127 |
| 2 | 181.4 | 131 | 201 | 129.6 | 80.6 | 188 |
| 2.5 | 187.2 | 142.6 | 213.5 | 131 | 103.7 | 210 |
| 3 | 207.4 | 207.4 | 341 | ---- | ---- | ---- |

The authors concluded that all three techniques were able to detect and provide quantitative size information. However, they ranked ultrasonics first, shearography second and ESPI third due to ease of operation and interpretation of results. They concluded that ultrasonics was the method of choice for

impact damage, but they always recommend that a second NDE method be used in conjunction with ultrasonics or destructive analysis to achieve higher acceptability and reliability in damage evaluation in critical applications.

4.3 Heat Damage

In the course of operations of both military and commercial aircraft and in other operations, composite materials may become weakened by thermal damage from jet blast, accidental fires and other heat sources. NDE techniques are needed to locate and evaluate this heat damage. For a detailed review of heat damage in graphite epoxy composites and applicable NDE techniques see Matzkanin and Hansen (1998). The author's major review covered the five major techniques used to detect heat damage in composites: thermal (IR), ultrasonics, acoustic emission, dielectric properties, and radiography. In addition, several other NDE techniques were reviewed.

Satish, et al. (2006) studied a novel, new technique for characterizing early stage or incipient heat damage in carbon fiber composites. They utilized a noncontact method based on the detection and measurement of heat developed during the propagation of an acoustic wave through the material. They stated that while NDE techniques based on ultrasonics, thermography and electromagnetics have been able to detect major heat damage in composites; they are not sensitive enough to detect incipient damage that will lead to greater damage as service is continued. Although, laser pumped fluorescence has shown capability to detect both major damage and incipient heat damage in composites, it is only applicable to surface damage. Figure 4.3.1 shows a schematic of the thermo-elastic material set up that the authors used. The noncontacting ultrasonic horn overcomes any potential problems with damage to the sample by direct contact with the horn. They studied carbon epoxy laminates with varying degrees of heat damage.

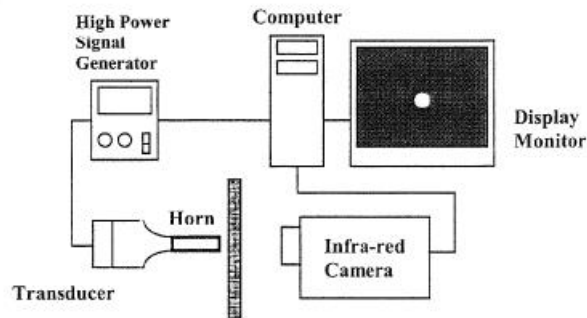


Figure 4.3.1. Block diagram of the thermo-elastic material characterization experimental set-up. (Satish, et al. 2006)

The authors conclude that their preliminary study indicated that incipient heat damage in carbon epoxy composites could be characterized by measuring the changes in the thermo-elastic property of the material.

Brady, et al. (2005) studied various heat-damaged samples of carbon-epoxy composite. They used proton NMR relaxation time measurement to try to locate and quantify the heat damage. In the first set of studies, the authors used traditional NMR equipment that required the samples to be placed inside of the NMF magnetic coil. This is in contrast to the second set of studies that utilized NMR equipment that allowed inspection to be one sided and suitable for aircraft inspection. The authors conclude that they could relate NMR measurements made with tradition equipment with heat damage. However, they concluded that measurements made with the one-sided NMR equipment had large measurement

uncertainties due to low signal to noise ratios and the results could not be related to the extent of heat damage.

4.4 Stress Rupture

Composite overwrapped pressure vessels (COPVs) are currently employed in such diverse applications as oxygen packs for fire fighters, oxygen storage for commercial and military aircraft, and fuel storage for transit buses. COPVs are also standard equipment for energy storage in numerous aerospace applications such as thrusters for station keeping on satellites and fuel pressurization on launch vehicles. Whenever gases are stored at high pressure in COPVs, the potential for stress rupture and the inadvertent release of the gas and the stored energy becomes an important safety issue.

Stress rupture is an insidious failure mode that occurs when fibers in a COPV are held at high stress for long periods of time, as is the case with COPVs kept at high internal pressure as described by L. Grimes-Ledesma, et al. (2006). Stress rupture is a global type of degradation that ultimately can result in catastrophic failure of the COPV. Stress rupture is not based on cyclic loading and has sometimes been referred to as static fatigue. COPV fibers creep under sustained high loads and this is thought to play a role in the stress rupture mechanisms. In addition, microcracking of the fibers has been identified as a potential failure mechanism. However the exact stress rupture failure mechanism for different types of fibers (Kevlar, Carbon, etc.) has not been fully defined.

Until 2006, there was very little information available on how to detect stress rupture degradation in COPVs using NDE. However, in 2006 NASA undertook a study to determine the feasibility of various NDE techniques to determine the degree of stress rupture degradation in Kevlar COPVs. This study is still ongoing, and the study is expected to be completed in 2008, private communication by authors of this Technology Assessment.

5.0 STANDARD PRACTICES IN INDUSTRY AND GOVERNMENT

5.1 Recent Development of Document Standards for NDE of Composites

5.1.1 Background

As indicated in the Introduction, there are a very limited number of document standards available for NDE of composites compared with document standards for the inspection of metals. However, there has been a great deal of research and development aimed at providing NDE techniques for the inspection of advanced composites used in aerospace applications. NASA recognized that in order to capture the benefits of these efforts and reliably apply these NDE techniques to plant and field inspection of composite aerospace components and systems, nationally recognized consensus document standards needed to be developed and promulgated. Based on this identified need for national consensus document standards for NDE of aerospace composites, in late 2004, NASA took the lead in initiating an effort to develop these needed standards. Although some technique oriented document standards were available for composites, application oriented, overarching document standards covering standard practices were lacking.

After discussion with the NASA representatives it was decided to pursue development of consensus standards under the auspices of ASTM International. ASTM has well developed procedures for writing national consensus standards which includes input and participation from all facets of the technical community, academia, industry, and government. In addition, ASTM Committee E07 on Nondestructive Testing has subcommittees that include experts in all the major NDE Techniques.

A Task Group was formed under ASTM Committee E07 on Nondestructive Testing to pursue development of document standards for NDE of aerospace composites. With input and participation from all facets of the technical community, academia, industry, and government, six ASTM International document standards have been written to date: a standard guide for NDE of aerospace composites and standard practices for acoustic emission, ultrasonics, shearography, thermography and radiography. Information is provided in this section on the current status of this effort and includes information on other document standards for NDE of advanced fiber reinforced polymer composites for use by industry and the government.

5.1.2 Standard Development Activities

The founding meeting of an ASTM Task Group for Development of Document Standards for the NDE of Aerospace Composites, took place on January 25, 2005 in conjunction with the ASTM E07 Committee Meeting in Ft. Lauderdale, FL. The meeting was attended by representatives from academia, the government and industry including major contractors, Boeing, Lockheed-Martin, and GE. Based on discussion at this meeting and subsequent telecons with other interested parties, it was decided to initially focus on polymer matrix composite systems with relatively simple geometries such as flat laminates.

Over the following months, a draft document standard was developed focusing on high performance polymer matrix composites using well established NDE techniques. This initial document took the form of an overarching standard guide for NDE of aerospace composites and was entitled, "Standard Guide for Nondestructive Testing of Polymer Matrix Composites Used in Aerospace Applications." The document was further discussed and developed at the June 2005 meeting of ASTM Committee E07 and the Task Group. Input to the document was sought from the various technical ASTM E07 subcommittees and other organizations interested in NDE of composites.

At the January 2006 meeting of the NDE of Composites Task Group, extensive discussion took place on the next steps for the Task Group. With encouragement from NASA, it was decided to embark on developing standard practices for NDE of aerospace composites. After several telecons over the following months and with input from others in the technical community, five technique-based standard practice documents were identified for development; these techniques were ultrasonics, acoustic emission, radiography, thermography, and shearography. At the June 2006 meeting of the Task Group and ASTM Committee E07, the relevant E07 technical expert subcommittees were requested to take the lead and join with the NDE of Aerospace Composites Task Group to write the five standard practice documents. Technical expert leads and sub task groups for each technique were identified and the five standard practice documents were written.

To date, three of the five standard practice documents discussed above have progressed through the ASTM consensus ballot process and have been published as ASTM standards. These are:

- E2581-07 "Standard Practice for Shearography of Polymer Matrix Composites, Sandwich Core Materials and Filament-Wound Pressure Vessels Used in Aerospace Applications."
- E2582-07 "Standard Practice for Infrared Flash Thermography of Composite Panels and Repair Patches Used in Aerospace Applications."
- E2580-07 "Standard Practice for Ultrasonic Testing of Flat Panel Composites and Sandwich Core Materials Used in Aerospace Applications."

The remaining two standard practice documents are currently progressing through the ASTM ballot process and are expected to be published as ASTM standards in 2008. These two are:

- “Standard Practice for Acoustic Emission Qualification of Plate-like and Flat Panel Composites Used in Aerospace Applications.” (In addition to this Standard Practice, a new companion Standard Guide for acoustic emission of composites is being developed).
- “Standard Practice for Radiography of Flat Panel Composites and Sandwich Core Materials Used in Aerospace Applications.”

In addition the “Standard Guide for Nondestructive Testing of Polymer Matrix Composites Used in Aerospace Applications” is also progressing through the ASTM ballot process and is expected to be published as an ASTM standards in 2008.

5.1.3 Future Work

At recent meetings of the ASTM NDE of Aerospace Composites Task Group extensive discussion took place on the next series of document standards to develop. Comments are summarized as follows:

- Move on to more complex polymer matrix composites, as a minimum, curved surfaces
- Composite overwrapped pressure vessels
- Brittle/ceramic matrix composites (RCC, etc.)
- Metal matrix composites

At the January 2008 meeting of the Task Group, based on the current needs of NASA, it was decided to pursue development of document standards for composite overwrapped pressure vessels (COPVs). As a result, a workshop on NDT of Composite Overwrapped Pressure Vessels is being planned for June 2008 in conjunction with the ASTM meetings in Denver, CO. The workshop is expected to culminate in a summary of COPV industry/user needs and capabilities for NDT of COPVS, and a draft road map for developing ASTM standard guides/practices/test methods and proficiency/interlaboratory crosscheck test programs.

5.2 Additional Document Standards for NDE of Composites

During the course of the work described above on developing document standards for NDE of aerospace composites, information was acquired on some existing standards for NDE of composites. For completion these are listed here. This is not intended to be an exhaustive list but to give an idea of other document standards for NDE of composites.

- ASTM/E1888 Test Method for Acoustic Emission Examination of Pressurized Containers Made of Fiberglass Reinforced Plastic with Balsa Wood Cores
- ASTM/E2191 Test Method for Examination of Gas-Filled Filament-Wound Composite Pressure Vessels Using Acoustic Emission
- ASTM/E1495 Guide for Acousto-Ultrasonic Assessment of Composites, Laminates, and Bonded Joints
- ASTM/E1736 Practice for Acousto-Ultrasonic Assessment of Filament-Wound Pressure Vessels
- ASTM/E1067 Practice for Acoustic Emission Examination of Fiberglass Reinforced Plastic Resin (FRP) Tanks/Vessels
- ASTM/E1570 Practice for Computed Tomographic (CT) Examination

SAE Aerospace Recommended Practices:

- ARP 5605 Solid Composite Laminate NDI Reference Standards
- ARP 5606 Composite Honeycomb NDI Reference Standards
- ARP 5089 Composite Repair NDT/NDI Handbook

The only NDE of composites standards currently in NASA books:

- MIL-HDBK-733 Nondestructive Testing Methods of Composite Materials-Radiography
- MIL-HDBK-787 Nondestructive Testing Methods of Composite Materials-Ultrasonic

6.0 CONCLUSIONS AND PROGNOSIS

Over the past twenty years, there has been a movement to use more composites in critical structural applications, as for example in commercial and military aircraft, composite overwrapped pressure vessels, and space systems. It is clear that this turn to composites for critical applications has accelerated remarkably over the past decade. Concurrent with the expanding use of composites in critical applications, there have been increasing requirements for NDE methods that can improve quality in composite manufacturing processes, end of manufacture quality/acceptance testing, and in-service inspection. These requirements have resulted in a very successful, broadly based research and development effort to meet the expanding needs for NDE in the composites arena.

The literature contains studies that have been successful for a very wide variety of NDE techniques applied to a wide variety of composite issues. However, many of these studies are lacking in producing quantitative capability information. In addition, structural designers that utilize composites for critical applications sometimes fail to provide the necessary quantitative accept/reject criteria for the various types of defects encountered in the composite structures they have designed. This lack of quantitative information extends to the lack of probability of detection (POD) information on NDE methods for composites. In addition, there are only a modest number of document standards that relate directly to NDE of composites. This lack of quantitative capability for NDE of composites is in sharp contrast to the very quantitative NDE methodology applied to metal structures.

In the opinion of the authors of this Technology Assessment, the NDE of composites community would provide a valuable service by focusing more heavily on the need for *quantitative* capability for NDE of composites. Quantitative studies on defect size and type versus NDE response, POD studies, development of document standards, and encouraging design engineers to provide quantitative accept/reject defect criteria for composite components are recommended. Of course, this type of information has already been developed by industry for some composites and applications, but most of it remains proprietary.

7.0 REFERENCES

D. P. Almond, S. K. Lau, "Defect Sizing by Transient Thermography. I. An Analytical Treatment." J. Phys. D: Appl. Phys., 27 1994, pp. 1063-1069.

- A. M. Amaro, J. B. Santos, and J. S. Cirne, "Comparative Study of Different Non-destructive Testing Techniques in the Characterization and Quantification of the Damage Effects in Carbon-epoxy Laminates." *Insight* Vol. 46, No. 9, September 2004, pp. 559-565.
- W. Bai, and B. S. Wong, "Evaluation of Defects in Composite Plates under Convective Environments using Lock-in Thermography." *Measurement Science and Technology*, Vol. 12, Institute of Physics Publishing, 2001, pp. 142-150.
- R.J. Ball, and D. P. Almond, "The Detection and Measurement of Impact Damage in Thick Carbon Fibre Reinforced laminates by Transient Thermography." *NDT&E International*, Vol. 31, No. 3. Elsevier Science, Ltd. 1998. pp. 165-173.
- Y. Bar-Cohen, Shyh-Shiuh Lih, "Experimental Enhancement of LLW Dispersion Data Acquisition and Implementation Challenges to NDE of Composites." *Materials Evaluation*, June 2000, Vol. 58 No. 6, pp. 801-806.
- P. J. Bierman, J. H. Crammer, C. A. Lebowitz, and L. M. Brown, "End-of-Cure Sensing using Ultrasonics for Autoclave Fabrication of Composites." *SPIE: Nondestructive Evaluation for Process Control in Manufacturing*, Vol. 2948, 1996, pp. 72-83.
- S. K. Brady, M. S. Conradi, and C.M. Vaccaro, "NMR Detection of Thermal Damage in Carbon Fiber Reinforced Epoxy Resins." *Journal of Magnetic Resonance*, Vol. 172, 2005, pp. 342-345.
- E. A. Brit, R. A. Smith, "A Review of NDE Methods For Porosity Measurement in Fiber-reinforced Polymer Composites." *Insight*, Vol 46, No 11, November 2004, pp. 681-686.
- H. J. Chun, P. S. Jang, "Nondestructive Evaluation of Degree of Fiber waviness in Thick Composites." *Key Engineering Materials*, Vols. 183-187, 2000, Trans Tech Publications, Switzerland, 2000, pp. 1069-1074
- A. Ciliberto, et al., "Porosity Detection in Composite Aeronautical Structures." *Infrared Physics & Technology*, Vol. 43, Issues 3-5, June 2002, pp. 139-143.
- A. R. Clark, G. Archenhold, N. C. Davidson, "A Novel Technique for Determining the 3D Spatial Distribution of Glass Fibres in Polymer Composites." *Composites Science and Technology*, Vol. 55. 1995. pp. 75-91.
- M. P. de Goeje, K. E. D. Wapenaar, "Nondestructive Inspection of Carbon Fibre-Reinforced Plastics Using Eddy Current Methods." *Composites*, Vol. 23, No. 3, May 1992, pp. 147-157.
- J. Degrieck, N. F. Declercq, O. Leroy, "Ultrasonic Polar Scans as a Possible Means of Nondestructive Testing and Characterization of Composite Plates." *Insight* 45, (3), pp. 196-201.
- D. J. Dorsey, R. Hebner, W. S. Charlton, "Nondestructive Evaluation of Carbon Fiber Composite Reinforcement Content." *Journal of Composite Materials*, Vol. 38, No. 17, pp. 1505-1519, 2004
- N. Elvin, C. Leung, "Feasibility Study of Delamination Detection with Embedded Optical Fibers." *Journal of Intelligent Material Systems and Structures*, Vol. 8. Technomic Publishing Co., Inc. 1998. pp. 824-828.

TEXAS RESEARCH INSTITUTE AUSTIN, INC.
A Texas Research International Company

D. Fei, D. K. Hsu, "Development of Motorized Azimuthal Scanners for Ultrasonic NDE of Composites." Annual Review of Progress in Quantitative Nondestructive Evaluation; Snowbird, UT; USA, July 19-24, 1998, pp. 1385-1392, 1999.

T. Gottesman, S. Girshovich, "Impact Damage Assessment and Mechanical Degradation of Composites." Key Engineering Materials, Vols. 141-143. Trans Tech Publications, Switzerland. 1998. pp. 3-18

L. Grimes-Ledesma, S. L. Phoenix, H. Beeson, T. Yoder, and N. Greene, "Testing of Carbon Fiber Composite Overwrapped Pressure Vessel Stress Rupture Lifetime." ACS/ASTM 21st Annual Technical Conference of the American Society for Composites, Dearborn, Michigan, September 17-20, 2006

E. G. Grinzato, S. Marinetti, P. G. Bison, "NDE of Porosity in CRFP by Multiple Thermographic Techniques." Proceedings of SPIE, Vol. 4710, Thermosense XXIV, March 2002, pp. 588-598.

X. E. Gros, K. Takahashi, "Nondestructive Characterization of Delaminated Areas at Interfaces Between Plies in Carbon Fiber/Epoxy Laminates with Foucault Currents." Composite Interfaces, Vol. 7, No. 3. VSP. 2000. pp. 177-192.

R. T. Harrold, R. Brynsvold, D. J. Hanko, "Embedded Acoustic Waveguides for Monitoring Composite Materials Processing and NDE." Proceedings of the 10th Annual ASM/ESD Advanced Composites Conference, Dearborn, Michigan, USA, November 1994, pp. 83-89.

R. B. Hesiehurst, J. P. Baird, and H. M. Williamson, "Location and Direction of the Propagation of an Existing Delamination in Composite Panels." Journal of Advanced materials, Vol. 30, No. 3 1998. pp. 38-43.

D. K. Hsu, "Ultrasonic Nondestructive Evaluation of Void Content in CFRP." ANTEC '88, Proceedings of the 46th Annual Technical Conference. 1988, pp. 1273-1275.

P. J. Joyce, D. Kugler, T. J. Moon, "A Technique for Characterizing Process-Induced Fiber Waviness in Unidirectional Composite Laminates-Using Optical Microscopy." Journal of Composite Materials, Vol. 31, No. 17, 1997, pp. 1694-1727

A. A. Karabuto, V. V. Murashov, N. B. Podymova, A. A. Oraevsky, "Nondestructive Characterization of Layered Composite Materials with a Laser Optoacoustic Sensor." Nondestructive Evaluation of Materials and Composites II, SPIE, Vol. 3396. Edited by Steven R. Doctor, Carol A. Lebowitz, and George Y. Baaklini. The International Society for Optical Engineering (SPIE). 1998. pp. 103.111.

Y. K. Kim, W. Zou, W. Sachse, "Wave Propagation in Wavy-Fiber Composite Material: Theory and Experiment." Journal of the Acoustical Society of America, May 1999, Vol. 103, Issue 5, pp. 2296-2301.

R. A. Kline, N. Parasnis, and R. Konanur, "Ultrasonic Monitoring of Cure in Composite Laminates." Review of Progress in Quantitative Nondestructive Evaluation, Vol. 13, 1994, pp. 2229-2236.

Lipetzky and Bandos (2003), K. G. Lipetzky and B. G. Bandos, "Composite Structures and Adhesive Joints: NDE Techniques for Naval Applications." SAMPE Journal, Vol. 39, No. 5, September/October 2003.

T. G. Marshall, Y. Hurmuzlu, "Detection and Quantification of Fiber Waviness in Thick Section Composite Components." AHS International Annual Forum, 55th, Montreal, Canada, Proceedings, Vol. 1, United States, 25-27 May 1999, pp. 818-824, 1999

- G. A. Matzkanin, G. P. Hansen, "Heat Damage in Graphite Epoxy Composites: Degradation, Measurement and Detection." A State-of-the-Art Report, NTIAC-SR-98-02, Sept. 1998.
- R. G. May, and R. O. Claus, "In-Situ Fiber Optic Sensor for Composite Cure Monitoring through Characterization of Resin Viscoelasticity." SPIE, Vol. 2948, pp. 24-34.
- A. Mian, X. Han, S. Islam, and G. Newaz, "Fatigue Damage Detection in Graphite/Epoxy Composites using Sonic Infrared Imaging Technique." Composites Science and Technology, Vol. 64. 2004. pp. 657-666.
- A. G. Miller, D. T. Lovell and J. C. Seferis, "The Evolution of an Aerospace Material: Influence of Design, Manufacturing and In-Service Performance." Composite Structures, 1994, Vol. 27. pp. 193-206.
- G. W. Mol, "Automated Estimation of Fiber Orientation of Cured CFRP by Image processing of High Resolution Ultrasonic Pulse-Echo Images." Nondestructive Testing 92, Edited by C. Halli and P. Kulcsar, Elsevier Science Publications B.V. 1992, pp. 979-983.
- J-W. Park, C-Y. Ryu, H-K. Kand, and C-S. Hong, "Detection of Buckling and Crack Growth in the Delaminated Composites using Fiber Optic Sensor." Journal of Composite Materials, Vol. 34, No. 19/2000. Technomic Publishing Co., Inc. 2000. pp. 1602-1623.
- W. J. Parker, R. J. Jenkins, C. P. Butler, G. L. Abbott, 1961. "Thermal Diffusivity Measurements Using the Flash Technique." J. Appl. Phys. 32 pp. 1679-1684.
- G. Petculescu, J. D. Achenbach, "Schedule Based NDT and Structural Health Monitoring of Safety Critical Composite Structures." Materials Evaluation, Vol. 65, No. 7, July 2007, pp. 731-739.
- G. Petculescu, S. Krishnaswamy, and J. D. Achenbach, "Evaluation of Delaminations and Impact Damage in Composites using the A Lamb Mode." Submitted for publication, 2007.
- B. P. Rice, C. W. Lee, "Novel, Low Cost Sensors for Intelligent Process Control." 41st International SAMPE Symposium, March 1996, pp. 1518-1529.
- M. O. W. Richardson, Z. Y. Zhang, M. Wisheart, J. R. Tyrer, J. Petzing, "ESPI Nondestructive Testing of GRP Composite Materials Containing Impact Damage." Composites, Part A 29A. Elsevier Science, Ltd. 1998, pp. 721-729.
- H. I. Ringermacher, D. R. Howard, "Synthetic Thermal Time-of-flight (STTOF) Depth Imaging," Review of Progress in Quantitative Nondestructive Evaluation, Vol. 20A, D. O. Thompson and D. E. Chimenti, eds., Melville, New York, AIP, 2001, pp. 487-491.
- S. Sathish, J. Welter, R. Reibel, and C. Buynak, "Thermo-elastic Characterization of Heat Damage in Carbon Fiber Epoxy Composites." CP820, Review of Quantitative Nondestructive Evaluation Vol. 25, ed. By D. O. Thompson and D. E. Chimenti, pp. 1015-1018.
- M. D. Seale, B. J. Smith, W. H. Prosser, J. N. Zalameda, "Lamb Wave Assessment of Fiber Volume Fraction in Composites." Journal of Acoustical Society of America, September 1998, Vol. 104, Issue 3, pp. 1399-1403.

- S. D. Sentura and N. F. Sheppard, "Dielectric Analysis for Thermoset Cure." *Advanced Polymer Science*, 80: pp. 1-47.
- D. D. Shepard, and K. R. Smith, "A Complete Ultrasonic Measurement System for In-process Cure Monitoring and Control of Composites." *Second Conference on NDE Applied to Process Control of Composite Fabrication*, NTIAC, 1996, pp. 61-68.
- S. M. Shepard, Y. L. Hou, T. Ahmed, J. R. Lhota, "Reference-free Interpretation of Flash Thermography Data," *Insight, British Inst NDT*, Vol. 48 No. 5, May 2006, pp. 298-301.
- J. S. Sirkis, C. C. Chang, and B. T. Smith, "Low Velocity Impact of Optical Fiber Embedded Laminated Graphite/Epoxy Panels. Part I: Macro Scale." *Journal of Composite Materials*, Vol. 28, No. 14/1994. Technomic Publishing Company, Inc. 1994. pp. 1347-1370.
- R. A. Smith, A. B. Marriott, and L. D. Jones, "Delamination Sizing in Fibre-Reinforced Plastics using Pulse-Echo Amplitude." *Insight*, Vol. 39, No. 5. May 1997. pp. 330-336.
- H. Songling, L. Luming, Y. Haiqing, S. Keren "NDE of Composites Delamination by Infrared Thermography." *NDE and Health Monitoring of Aerospace Materials and Composites II*, Andrew L. Gykenyesi, Peter J. Shull, Editors, *Proceedings of SPIE Vol. 5046*, 2003. pp. 219-223.
- K. V. Steiner, "Defect Classifications in Composites Using Ultrasonic Nondestructive Evaluation Techniques." *Damage Detection in Composite Materials*, STP 1128. Edited by John E. Masters. Philadelphia, PA: American Society for Testing and Materials (ASTM). 1992. pp. 72-84.
- K. V. Steiner, et al., "Infrared Thermography and Laser-Based Ultrasonic Methods for On-Line Porosity Sensing During Thermoplastic Composite Fabrication." *Second Conference on NDE Applied to Process Control of Composite Fabrication*, NTIAC, 1996, pp.115-122.
- S. Sugimoto, E. Aoki, Y. Iwahora, T. Ishikawa, "Nondestructive Evaluation of Composites Using Micro-Focus X-ray Scanner." *Review of Quantitative Nondestructive Evaluation*, Vol. 24, ed. By D. O. Thompson and D. E. Chimenti, American Institute of Physics, 2005, pp. 1081-1086.
- R. W. Sullivan, K. Balasubramaniam, G. Bennett, "Plate Wave Flow Patterns for Ply Orientation Imaging in Fiber Reinforced Composites." *Materials Evaluation*, Vol. 54, No. 4, April 1996. pp. 518-523.
- A. Todoroki, H. Kobayashi, and K. Matsuura, "Application of Electric Potential Method to Smart Composite Structures for Detecting Delamination." *Proceedings of ICCM-10*, Whistler, B.C. Canada. August 1995. pp. V323-V330.
- H. Voillaume, D. Simonet, C. Brousset, P. Barbeau, J-L. Arnaud, M. Dubois, T. Drake, M. Osterkamp, "Analysis of Commercial Aeronautics Applications of Laser Ultrasonics for Composite Manufacturing," *Proceedings of ECNDT 2006*, 9th European Conference on NDT, Berlin, Germany, September 25-29, 2006, pp. 1-8.
- X. Wang, and D. D. L. Chung, "Sensing Delamination in a Carbon Fiber Polymer-Matrix Composite During Fatigue by Electrical Resistance Measurement." *Polymer Composites*, Vol. 18, No. 6. 1997. pp. 692-700.

TEXAS RESEARCH INSTITUTE AUSTIN, INC.
A Texas Research International Company

W. Weigl, D. Findeis, E. Schnack, and J. Gryzagoridis, "Comparing Optical Interference Techniques for the Nondestructive Detection of Delaminations in Layered Composites." Proceedings of the Seventh International Conference on Composites Engineering, ICCE7, Denver, CO, 2000, pp. 921-922.

S. C. Wooh, I. M. Daniel, "Characterization of Fiber Waviness in Thick Section Composites Based on Ray Tracing Model." Review of Progress in Quantitative Nondestructive Evaluation, Vol. 13, Edited by D. O. Thompson and D. E. Chimenti, Plenum Press, New York, 1994, pp. 1291-1298.

L. Yang, "Recent Developments in Digital Shearography for Nondestructive Testing." Materials Evaluation, 2006, Vol. 64, No. 7. pp. 704-709.

J. N. Zamaleda, W. P. Winfree, "Quantitative Thermal Diffusivity Measurements on Composite Fiber Volume Fraction (FVF) Samples." Review of Progress in Quantitative Nondestructive Evaluation, Vol. 12B, Edited by Donald O. Thompson and Dale E. Chimenti. New York: Plenum Press 1993, pp. 1289-1295.

J. N. Zalameda, and B. T. Smith, "Measurement of Composite Fiber Volume Fraction using Thermal and Ultrasonic Inspection Techniques." Nondestructive Characterization of Materials VI. Edited by R. E. Green, Jr., Krzysztof J. Kozaczek, and Clayton O. Ruud. New York: Plenum Press. 1994. pp. 741-748.

| REPORT DOCUMENTATION PAGE | | | Form Approved OMB No. 0704-0188 | | |
|---------------------------------------------------------------------------------------------------------------------------------------------------------------------------------------------------------------------------------------------------------------------------------------------------------------------------------------------------------------------------------------------------------------------------------------------------------------------------------------------------------------------------------------------------------------------------------------------------------------------------------------------------------------------------------------------------------------------------------------------------------------------------------------------------------------------------------------------------------------------------------------------------------------------------------------------------------------------------|-------------|-------------------------------------|---------------------------------------------------------------|------------------------------|-------------------------------------------------------------|
| <p>The public reporting burden for this collection of information is estimated to average 1 hour per response, including the time for reviewing instructions, searching existing data sources, gathering and maintaining the data needed, and completing and reviewing the collection of information. Send comments regarding this burden estimate or any other aspect of this collection of information, including suggestions for reducing this burden, to Department of Defense, Washington Headquarters Services, Directorate for Information Operations and Reports (0704-0188), 1215 Jefferson Davis Highway, Suite 1204, Arlington, VA 22202-4302. Respondents should be aware that notwithstanding any other provision of law, no person shall be subject to any penalty for failing to comply with a collection of information if it does not display a currently valid OMB control number. PLEASE DO NOT RETURN YOUR FORM TO THE ABOVE ADDRESS.</p> | | | | | |
| 1. REPORT DATE (DD-MM-YYYY) 01-02-2009 | | 2. REPORT TYPE Contractor Report | | 3. DATES COVERED (From - To) | |
| 4. TITLE AND SUBTITLE Nondestructive Evaluation of Advanced Fiber Reinforced Polymer Matrix Composites - A Technology Assessment | | | 5a. CONTRACT NUMBER NNL07AA00B | | |
| | | | 5b. GRANT NUMBER | | |
| | | | 5c. PROGRAM ELEMENT NUMBER | | |
| 6. AUTHOR(S) Yolken, H. Thomas; Matzkanin, George A. | | | 5d. PROJECT NUMBER | | |
| | | | 5e. TASK NUMBER NNL07AM00T | | |
| | | | 5f. WORK UNIT NUMBER 939904.05.07 | | |
| 7. PERFORMING ORGANIZATION NAME(S) AND ADDRESS(ES) NASA Langley Research Center Hampton, VA 23681-2199 | | | 8. PERFORMING ORGANIZATION REPORT NUMBER | | |
| 9. SPONSORING/MONITORING AGENCY NAME(S) AND ADDRESS(ES) National Aeronautics and Space Administration Washington, DC 20546-0001 | | | 10. SPONSOR/MONITOR'S ACRONYM(S) NASA | | |
| | | | 11. SPONSOR/MONITOR'S REPORT NUMBER(S) NASA/CR-2009-215566 | | |
| 12. DISTRIBUTION/AVAILABILITY STATEMENT Unclassified - Unlimited Subject Category 38 Availability: NASA CASI (443) 757-5802 | | | | | |
| 13. SUPPLEMENTARY NOTES Langley Technical Monitor: Erik I. Madaras | | | | | |
| 14. ABSTRACT Because of their increasing utilization in structural applications, the nondestructive evaluation (NDE) of advanced fiber reinforced polymer composites continues to receive considerable research and development attention. Due to the heterogeneous nature of composites, the form of defects is often very different from a metal and fracture mechanisms are more complex. The purpose of this report is to provide an overview and technology assessment of the current state-of-the-art with respect to NDE of advanced fiber reinforced polymer composites. | | | | | |
| 15. SUBJECT TERMS Cure monitoring; Delaminations; Fiber/matrix flaws; Heat damage; Impact damage; NDE; Polymer matrix composites; Porosity; Stress rupture | | | | | |
| 16. SECURITY CLASSIFICATION OF: | | | 17. LIMITATION OF ABSTRACT | 18. NUMBER OF PAGES | 19a. NAME OF RESPONSIBLE PERSON |
| a. REPORT | b. ABSTRACT | c. THIS PAGE | | | STI Help Desk (email: help@sti.nasa.gov) |
| U | U | U | UU | 56 | 19b. TELEPHONE NUMBER (Include area code) (443) 757-5802 |